Friedrich-Schiller-Universität Jena
Chemisch-Geowissenschaftliche Fakultät

Tracking photosynthetically fixed carbon into soil microbial groups using lipid biomarkers

Masterarbeit

Zur Erlangung des akademischen Grades
„Master of Science“ (M.Sc.)
im Studiengang
„Biogeowissenschaften“

Vorgelegt von: Helena Lisa Dannert
Matrikelnummer: 131729
Abgabedatum: 10. Januar 2014
Erstgutachterin: Prof. Dr. Erika Kothe (Friedrich-Schiller-Universität Jena)
Zweitgutachter: Prof. Dr. Gerd Gleixner (MPI Jena)

Acknowledgment

This master thesis has been carried out at the Max Planck Institute of biogeochemistry in Jena. A number of people deserve thanks for their help and support. It is therefore my pleasure to express my gratitude to them all in this acknowledgement.

I would like to thank Prof. Dr. Gerd Gleixner for giving me the opportunity to conduct my study in his working group. I also thank him for his support in scientific questions and his comments. I wish to thank also my supervisor Ashish Malik for the opportunity to work within his project and for his useful comments, remarks and engagement throughout the writing process. Also, I like to thank Steffen Rühlow who supported me with his technical knowledge. Furthermore I would like to thank the whole working group for supporting me with their experiences.

Abstract

Within the terrestrial system soil is the main C reservoir. The release of photosynthetically assimilated carbon into soil regulates microbial biomass. Large contributors to soil carbon are Arbuscular mycorrhizal fungi, which are suggested to play an important role in the carbon cycle of soil. Little is known about details of carbon cycling processes in soil and the role of different microbial groups in it. Better insights into belowground processes of carbon are needed. Microbial community phospholipid fatty acids (PLFAs) and neutral lipid fatty acids (NLFAs) analyses and stable isotope labeling experiment were combined to identify soil microbial groups involved in incorporation of photosynthetically fixed carbon. Pulse-chase labeling with $^{13}CO_2$ was performed in greenhouse chambers with *Chenopodium ambrosioides,* a plant which is known for its AMF symbiosis. Time course sampling was done within hours to weeks after labeling to investigate the temporal dynamics of assimilated carbon into different microbial groups. The extracted lipids from soil were measured with a GC-FID system for quantification and with a GC-c-IRMS system for isotope analysis. ^{13}C enrichment of PLFAs occurred already immediately after the labeling, but temporal differences were found across microbial groups. Saprophytic fungi, AMF and general biomarkers (18:2ω6,9, 16:1ω5 NLFA, n16:0) showed the highest and fastest enrichment as did the Gram-negative bacterial monounsaturated molecular markers (16:1ω7 and 18:1ω7). In comparison, the Gram-positive bacteria and Actinomycetes had very small ^{13}C enrichment that appeared later during the sampling period. These results indicate a fast C flux from plants into fungal communities and a delayed processing of plant carbon by bacteria, suggesting the use of dead roots and fungal necromass by Gram-positive bacteria. Additionally two different feeding strategies of bacteria could be identified. Gram-positive bacteria and Actinomycetes employed the saprophytic pathway whereas Gram-negative bacteria (monounsaturated biomarkers 16:1ω7 and 18:1ω7) seem rely on direct plant root exudates. These results suggest an important role of fungi and bacteria in the carbon cycle of soil.

Kurzfassung

Der Boden ist das größte Kohlenstoffreservoir im terrestrischen System. Mikrobielle Biomasse im Boden wird durch die Freisetzung von photosynthetisch aufgenommenem Kohlenstoff reguliert. Ein großer Beitrag des Kohlenstoffs im Boden wird durch Arbuskuläre Mykorrhizapilze geleistet, welche eine bedeutende Rolle im Kohlenstoffkreislauf spielen. Es ist bisher wenig über Details des Kohlenstoffzyklus im Boden und die Rolle der verschiedenen mikrobiellen Gemeinschaften bekannt. Tiefere Einblicke in die Prozesse im Boden sind nötig, um den komplexen Kohlenstoffkreislauf zu verstehen. Ein $^{13}CO_2$ pulse-chase Label Experiment wurde an einem Pflanzen-Boden System durchgeführt und Isotope von Phosphorlipiden und Neutrallipide von mikrobiellen Organismen wurden analysiert, um spezifische mikrobielle Gemeinschaften mit der Aufnahme des Kohlenstoffs zu verknüpfen. Hierzu wurden *Chenopodium ambrosioides* Pflanzen genutzt, die eine Symbiose mit Mykorrhizapilze eingehen. Bodenproben wurden an zehn verschiedenen Zeitpunkten innerhalb von wenigen Stunden bis hin zu mehreren Wochen nach dem Labeln genommen, um den zeitlichen Verlauf der Kohlenstoffaufnahme zu verfolgen. Die extrahierten Lipide wurden anhand von einem GC-FID System zur Quantifizierung gemessen und mit einem GC-c-IRMS wurden Isotopenwerte bestimmt. Die Anreicherung von ^{13}C in spezifischen Lipiden tritt sofort nach dem Labeln auf. Es wurden zeitliche unterschiede der Aufnahme in die verschiedenen mikrobiellen Gemeinschaften beobachtet. Die größte und schnellste Aufnahme des ^{13}C wurde in Biomarkern der saprophytischen Pilze, AMF und der ganzen Bodengemeinschaft (18:2ω6,9, 16:1ω5 NLFA, n16:0) gefunden. Auch einfach ungesättigte Lipide der Gram-negativen Bakterien weisen eine schnelle Anreicherung auf. Im Vergleich haben Gram-positive Bakterien und Aktinomyzeten die geringste Anreicherung und weisen eine zeitlich versetzte Anreicherung auf. Diese Ergebnisse weisen auf einen schnellen Prozess des Kohlenstoffs von den Pflanzen zu den Pilzgemeinschaften im Boden und einem späteren Transfer des Kohlenstoffs zu bakteriellen Gemeinschaften hin. Das kann einem Transport von Pilzen zu den Bakterien zugeschrieben werden oder der Bevorzugung von toten Wurzeln und Pilznekromasse als Nahrung der Bakterien. Zusätzlich konnten zwei verschiedene Nahrungsstrategien der Bakterien in den analysierten Bodenproben identifiziert werden: Gram-positive Bakterien und Aktinomyzeten ernähren sich saprophytisch, wohingegen Gram-negative Bakterien (mehrfach ungesättigte Biomarker 16:1ω7 und 18:1ω7) von pflanzenverfügbaren Kohlenstoffkomponenten abhängig zu sein scheinen. Diese Ergebnisse weisen auf eine wichtige Rolle von Pilzen und Bakterien im Kohlenstoffkreislauf im Boden hin.

Index

I. List of figures i

II. List of tables ii

III. List of abbreviation iii

1 Introduction 1

1.1 Carbon cycle in soil 1

1.2 Stable isotope technologies and biomarkers 2

2 Materials and Methods 5

2.1 Plant and soil study system 5

2.2 $^{13}CO_2$ pulse-chase labeling 5

2.3 Soil sampling 5

2.4 Biomarker extraction 6

2.4.1 Lipid extraction 6

2.4.2 Separation of lipids 6

2.4.3 Mild alkaline hydrolysis (plus methylation): 7

2.4.4 Separation of unsubstituted FAMEs 7

2.4.5 Separation of unsubstituted ester linked PLFAs 7

2.5 Measurement of the samples 8

2.5.1 Gas chromatograph coupled with flame ionization detector 8

2.5.2 Isotope-ratio mass spectrometer 9

2.6 Statistical analysis 10

3 Results 11

3.1 Biomarkers 11

3.2 Soil community composition 12

3.3 Lipid incorporation of photosynthetically fixed ^{13}C 14

3.4 Fungal lipid biomarkers 15

3.4.1 Saprophytic and general fungi 15

3.4.2 Arbuscular mycorrhiza fungi 17
3.5 Bacterial lipid biomarkers 19
3.5.1 Gram-positive bacteria 19
3.5.2 Gram-negative bacteria 20
3.5.3 Actinomycetes 22
3.6 General biomarkers 23
4 Discussion 25
4.1 Data review 25
4.2 Microbial community composition 25
4.3 Pool origin of the biomarkers 26
4.4 Lipid biomarkers specific ^{13}C enrichment 28
4.4.1 Fungal lipid biomarkers 29
4.4.2 Bacterial lipid biomarkers 30
4.5 Duration of ^{13}C enrichment of specific biomarkers 32
4.6 Environmental inferences from carbon utilization 34
5 Conclusion 35
6 References 37
7 Appendix 41

I. List of figures

Figure 1: GC-IRMS chromatogram of sample T1 A. 11
Figure 2: PCA of the PLFA composition from all samples. 12
Figure 3: Mean concentration of analyzed PLFAs. 13
Figure 4: NLFA 16:1ω5 concentration in the samples.. 14
Figure 5: Saprophytic fungal biomarker ^{13}C enrichment. 15
Figure 6: General fungal biomarker ^{13}C enrichment. 16
Figure 7: Arbuscular mycorrhizal fungi PLFA biomarker ^{13}C enrichment. 17
Figure 8: Arbuscular mycorrhiza fungi NLFA biomarker ^{13}C enrichment. 18
Figure 9: Gram-positive bacterial biomarkers ^{13}C enrichment. 19
Figure 10: Gram-negative bacterial biomarkers ^{13}C enrichment. 20
Figure 11: Actinomycetes biomarker ^{13}C enrichment 22
Figure 12: Communitiy biomarker ^{13}C enrichment. 23
Figure 13: Nonspecific biomarker ^{13}C enrichment. 24
Figure 14: Distribution of the concentration of different microbial groups. 25
Figure 15: Excess ^{13}C of specific organism groups. 29
Figure 16: Bulk ^{13}C enrichment of the microbial communities. 33

Figure A1: Boxplot of the NLFA concentrations 52

II. List of tables

Table 1: Soil sampling time points. 6
Table 2: Characteristic fatty acid lipids as indicators for different organism sources. 11
Table 3: Concentration of the total, bacterial and fungal biomass in the soil samples 13
Table 4: Correlation matrix of the ^{13}C enrichment values of the different analyzed microbial biomarkers. 26

Table A 1: Weigh determination of the different parameters for each sample. 41
Table A 2a-c: Concentration of all detected PLFAs in mol%. 42
Table A 3a-c: Concentration of the analyzed PLFAs and NLFAs in mol g^{-1} 45
Table A 4a-c: Isotopes values after offset correction. 48
Table A 5a-b: ^{13}C enrichment in C nmol g^{-1}. 51

III. List of abbreviation

AMF	Arbuscular mycorrhizal fungi
C	Carbon
$CHCl_3$	Chloroform
CO_2	Carbon dioxide
DCM	Dichloromethane
FID	Flame ionization detector
GC	Gas chromatograph
GC-c-IRMS	Gas chromatograph-combustion-isotope-ratio mass spectrometer
M	Molar
MeOH	Methanol
MUFA	Monounsaturated fatty acids
N	Nitrogen
PCA	Principal component analysis
PLFA	Phospholipid fatty acid
PUFA	Polyunsaturated fatty acid
RDA	Redundancy analysis
SATFA	Saturated fatty acid
SF	Saprophytic fungi
SIP	Stable isotope probing
SOC	Soil organic carbon
VPDB	Vienna Pee-Dee-Belemnite

1 Introduction

The carbon (C) cycle is an important topic in today's ecology, oceanography and geochemical research since the level of atmospheric carbon dioxide (CO_2) has increased over the past 120 years due to anthropogenic inputs (Schimel, 1995). Especially since industrialization the CO_2 level is increasing fast due to anthropogenic CO_2 emissions (for example burning fossil fuels and aerosols) (Mooney et al., 1991). The fast rising CO_2 level over the last decades and the awareness of its consequences makes the understanding of carbon cycle a crucial topic. Carbon cycling takes place between five main pools; the oceanic pool, fossil fuel reserves, pedologic pool, atmospheric pool and biotic pool (Lal, 2008). The pedologic pool is the third largest carbon pool and together with the biotic pool makes the terrestrial pool. Enormous research efforts have been made to get insights into the carbon cycle and in understanding the exchange between the different C pools. Within the carbon cycle the terrestrial pool plays a big role in carbon sequestration; storage of CO_2 in living and dead organic matter makes it a big carbon sink (Lal, 2008). The atmospheric pool interacts strongly with the terrestrial pool through photosynthesis, a process by which atmospheric CO_2 is fixed by plants and autotrophic microbes. This process regulates the carbon flow in soil system and is one of the key processes in terrestrial ecosystems (van Veen et al., 1989). The soil system is the largest reservoirs of organic carbon in the terrestrial biosphere (Cardon et al., 2001). Since the soil carbon cycle is a critical regulator of the global carbon budget (Johnston et al., 2004) it is imperative to better understand the carbon flux from atmosphere into the belowground microbial communities. The work presented in this thesis is aimed in improving this understanding.

1.1 Carbon cycle in soil

Soil organic carbon (SOC) is the largest pool within the terrestrial C cycle (Kandeler et al., 2005). The input of photosynthetically fixed carbon into soil occurs through aboveground litter fall and belowground rhizodeposition by plants (Kandeler et al., 2005). Rhizodeposition includes several C flow processes from plants to soil: (1) root cap and border cell loss, (2) death and lysis of root cells, (3) flow of C to root-associated symbionts living in the soil (4) gaseous losses, (5) leakage of solutes from living cells and (6) insoluble polymer secretion from living cells (Jones et al., 2009). Soil is a complex ecosystem generally containing a high biodiversity. In the rhizosphere easily degradable carbon sources became available. The rhizosphere is known for both high biodiversity and high biomass in comparison to the bulk soil. Microbes colonize the rhizosphere because of the root derived carbon, which is the main energy source for microorganisms that is used for catabolic and biosynthetic processes (Drigo et al., 2010). In turn, plants benefit from the decomposition of organic material by the microbes that provides the plants important nutrients (Lynch and Whipps, 1990). The soil

micro fauna has an important influence on energy and carbon flow through the terrestrial system and are key components of the food web (Scheu et al., 2005). Microorganisms are primary regulators of nutrient cycling and decomposition of plant provided material (Williams et al., 2006). Fungi are important drivers of microbiological and ecological processes in soil e.g. influencing soil fertility, substrate decomposition, cycling of minerals (Finlay, 2008). Arbuscular Mycorrhizal fungi (AMF) are the most ancient fungal symbioses found in plant systems, occurring in about two-third of all land plants (Jones et al., 2004). They are large contributors to soil microbial biomass (Olsson, 1999). AM fungi colonize plant roots and rely on the plant host for its carbon requirement (Johnson et al., 2002). They are revealed to play a major role in soil carbon cycle (Finlay, 2008). The plant rhizosphere AMF network is surrounded by colonies of rhizosphere bacteria (Frey-Klett et al., 2007). Recent studies demonstrate a rapid pathway of carbon from plants via AMF into the soil and back to the atmosphere (Johnson et al., 2002). Furthermore the carbon from AMF is released into surrounding bacterial and fungal groups (Drigo et al., 2010). It is known that plants allocate up to 30 % of their fixed carbon to AMF and this carbon is transferred to other soil microbes. AMF had been demonstrated as the major conduit in the transfer of carbon from plants to soil (Drigo et al., 2010). However, little is known about the mechanisms regulating belowground soil carbon cycling. The lack of understanding is due to technological difficulties in studying the soil system, which is complex and dynamic and is altered by changing environment (Johnston et al., 2004). The knowledge of microbial groups involved in soil carbon cycling is limited due to the lack of cultivability of microorganisms. Less than 1 % of soil microorganisms are cultivable (Torsvik et al., 1990). Therefore culture experiments are limited to studying the cultivable microorganisms that represent only a minor fraction of the total community (Kreuzer-Martin, 2007). This makes it imperative to use technical approaches that allow investigation of the total microbial community which would help gain a better insight into their processes. A number of culture independent techniques coupled with stable isotopes analysis are now used in microbial ecology studies (Boschker and Middelburg, 2002).

1.2 Stable isotope technologies and biomarkers

The development of culture-independent molecular biological tools advanced the research of understanding of belowground microbial processes. Stable isotopes have been widely used to identify nutrient sources in the past several decades (Ehleringer et al., 2000, Kreuzer-Martin, 2007). 98.9 % of C in nature exists as ^{12}C as against only 1.1 % of ^{13}C (Glaser, 2005). Isotopic differences occur during kinetic and thermodynamic processes, where the lighter isotopes are preferred to the heavier ones (Glaser, 2005). Different carbon pools are affected differentially by isotopic fractionation processes and therefore have specific isotopic

composition. Kinetic fractionation is caused by higher mobility of lighter isotopes. Carbon molecules are incorporated into biomass during multi step anabolic processes that lead to fractionation of the isotopes. Usually there is a discrimination against ^{13}C during such biosynthesis because the uptake of ^{12}C costs less energy due to the lower molecular weight (Farquhar et al., 1989). This knowledge can be used to comprehend processes in uptake of substances.

An ongoing challenge is to link specific organisms in the environment to their metabolic activities (Kreuzer-Martin, 2007). Stable isotope probing (SIP) has been used as an approach to link specific microbial communities with biogeochemical processes (Lu et al., 2007). The use of compound specific stable isotope analysis enables investigations of (1) microbial processes and trophic relationships between organisms, (2) to quantify sequestration and turnover of specific substances, and (3) to trace origin of substances (Glaser, 2005). One such method involves measurement of lipids using Gas chromatography-combustion-Isotope ratio mass spectrometry (GC-c-IRMS) (Boschker and Middelburg, 2002). Several compounds are used in organic geochemistry to detect different groups of organisms in environmental samples (Boschker and Middelburg, 2002). These called biomarkers which are organic compounds with a taxonomic relationship to specific microbial groups. In microbial ecology interrogations phospholipid fatty acids (PLFAs) have been revealed as useful biomarkers. PLFAs are membrane components of all living cells and are mineralized rapidly after cell death; and therefore represent the active microbial community (Zelles et al., 1992, Zelles, 1999). Different microbial groups have characteristic PLFA patterns and are therefore suitable as biomarkers (Boschker and Middelburg, 2002, Glaser, 2005). PLFA analysis is a biochemical method that provides direct information about the structure of the active microbial community (Bossio and Scow, 1998). PLFA profiles give information about community structure and their changes due to environmental effects. Functional information of microbial communities can be provided by substrate utilization examinations. Using stable-isotope labeled microbial substrates it is possible to track the path of the substrate into the active microbial community by analyzing specific biomarker molecules (Kreuzer-Martin, 2007). This approach removes the need to consider isotopic fractionation, as the ^{13}C pulse is generally many orders of magnitude greater than any fractionation that may occur (Ruess and Chamberlain, 2010). SIP has been used to study C dynamics in soil and to follow photosynthetically fixed C into microorganisms (Rattray et al., 1995). Several studies have used stable isotope labeling approaches in combination with PLFA analysis, which have improved our understanding of carbon flow through different trophic levels in soil systems. Stable isotope label can be applied to a soil system by direct input of ^{13}C enriched substrate or indirectly through photosynthetic uptake of enriched CO_2 by vegetation (Treonis et al., 2004). In one study ^{13}C-labeled substrate was added into sediment cores to demonstrate that acetate was

primarily used by sulphate-reducing bacteria (Boschker et al., 1998). Also ^{13}C labelled plant residues can be applied to soil to determine C flow (Williams et al., 2006). Another possibility is to conduct a pulse labeling experiment of plants with enriched $^{13}CO_2$. Butler et al. (2003) conducted a pulse labeling of plants and showed differences in rhizodeposition pattern during different stages of plant development. In several studies it was shown that either AMF or general fungi get a rapid ^{13}C enrichment in pulse-chase labeling experiments (Butler et al., 2003, Denef et al., 2007, Drigo et al., 2012). Results from these studies showed a strong relationship of plants and belowground microbial communities. Further research is necessary to get insights into temporal characteristics of C dynamics in soil.

The objective of the present study was to use the $^{13}CO_2$ pulse-chase labelling technique and fatty acid analysis to track photosynthetically fixed ^{13}C into the belowground microbial food web and study the temporal pattern of carbon uptake into different microbial groups in an AMF soil system. A pot experiment was conducted using *Chenopodium ambrosioides*, which forms a symbiotic association with AMF. The experiment was conducted at the Max Planck Institute for Biogeochemistry in Jena in the working group “Molecular Biogeochemistry” of Prof. Dr. Gerd Gleixner. The master thesis is a part of Ashish Malik´s PhD project. Plants were labeled with $^{13}CO_2$ and the soil was analyzed for fatty acids. A time series sampling was done over a period of a month to study the temporal dynamics and shifts in microbial community ^{13}C incorporation. Special focus was on the role of AMF in the carbon cycle of soil. We hypothesize that ^{13}C enrichment will temporally vary among microbial groups. AMF and fungal biomarkers are likely to incorporate C from the rhizodeposits first and are thought to be the main drivers of the photoassimilated carbon. We hypothesize further that AM fungi play the most dominant role in the carbon transfer and bacteria on the contrary play a minor role in this initial carbon flux from plants to soil microorganisms. Furthermore carbon uptake patterns of individual biomarkers thought to be used as indicators for environmental behavior of the specific microorganisms.

2 Materials and Methods

2.1 Plant and soil study system

For the experiment soil from the Jena Biodiversity Experiment site located in Jena, Germany was collected in September 2012. The soil was characterized as slightly sandy. Soil was sieved <2 mm and all visible roots were picked manually to have no prior signals. Homogenized soil was stored at 4°C until it was planted. 1L polystyrene pots were filled with 700 g of soil and placed in the greenhouse with additional light (Son-T Agro 430 W HPS bulbs, primary light range = 520-610 nm, Philips Lighting Company, New Jersey, USA) for 12 hours during the day. The pots were uniformly watered with an automated irrigation system that delivered water two to three times per day for three minutes each. Seeds of *Chenopodium ambrosioides* were sown into the pots after 2 weeks of soil acclimatization. *C. ambrosioides* is a temperate herb that is known to form mycorrhizal association. The plants were grown for four weeks until true leave growing and they were redistributed with a frequency of three plants per pot. Plants were allowed to grow in the greenhouse for 3 months.

2.2 $^{13}CO_2$ pulse-chase labeling

The labeling experiment took place at the greenhouse of the Max Planck Institute for Biogeochemistry in Jena, Germany. After the growth period of three month the planted pots were allocated into CO_2 plexiglass gas flow chambers of 2000 L, using three replicates per sampling point (29 labeled, loss of one pot). Three pots were maintained as unlabeled control pots. Prior to introduction of $^{13}CO_2$, the chamber was flushed with CO_2 free synthetic air until the concentration of CO_2 fell below 50 ppm. 99 atom% ^{13}C enriched CO_2 was introduced into the labeling chamber at a flow rate of 100 ml/min and was cycled throughout the chamber using an internal ventilation system to achieve uniform labeling. Photosynthetic uptake was monitored and throughout the labeling period of 10 h, the CO_2 concentration in the chamber was maintained between 350-400 ppm. Photosynthetic rate was around 100 ppm/h at the beginning and dropped below 50 ppm/h towards the end of the labeling period. At the end of the labeling period (10 h), the chamber was opened, and the plants were returned to the greenhouse.

2.3 Soil sampling

Soil sampling was done at ten different time points (Table 1). Each sampling point had three plant system replicates (A, B and C). The pots were heavily colonized by plant roots hence, after discarding the top 5 cm the rest of the soil was considered as rhizosphere soil. Additionally three unlabeled control replicates were sampled prior the pulse labeling to serve as

control for background $\delta^{13}C$ values. The samples were sieved <2 mm and roots were picked manually to have no plant and root signals. The soil was stored in bags at -20°C until the extraction.

Table 1: Soil sampling time points.

Sample Code	Sampling Point
T1 (A,B,C)	Immediately
T2 (A,B,C)	3 hours
T3 (A,B,C)	12 hours
T4 (A,B,C)	24 hours
T5 (A,B,C)	48 hours
T6 (A,B,C)	96 hours
T7 (A,B,C)	1 week
T8 (A,B,C)	2 weeks
T9 (A,B,C)	3 weeks
T10 (A,B)	4 weeks
CON (A,B,C)	Unlabeled/before

2.4 Biomarker extraction

2.4.1 Lipid extraction

Approximately 50 g dry weight of soil samples (Table A 1) were extracted according to a modified Bligh and Dyer extraction (Bligh and Dyer, 1959). The lipids were extracted with a mixture of chloroform ($CHCl_3$), methanol (MeOH) and a 0.05 Molar (M) phosphate buffer (pH 7.4) (1:2:0.8; v:v:v). To determine the buffer amount for each sample the water content of the samples were determined and subtracted from 50 ml of the buffer.

$$\text{Buffer (ml)} = \frac{50 - (\text{water content} \times \text{soil wet weight})}{100}$$

The samples were stored for two days in the fridge. During this time the water and the methanol solution got separated from the chloroform. Two phases were built and the soil got deposited at the bottom. Afterwards the water and MeOH layer is removed and the soil mixture is filtered with Celite 454. This filtrate collected contains the extracted lipids. The filtrate is reduced to a volume of 10 mL. This product at this stage is a stable intermediate and can be stored over a long period in the freezer (-20°C).

2.4.2 Separation of lipids

The obtained lipids were separated into neutral lipids, phospholipids and glycolipids on silica columns. The columns had a size of 2 g/12 mL and were conditioned with 1 V of Chloroform. 3 mL of the extract was put onto the column and discarded. To collect the neutral lipids 1 V

of chloroform was added to the extract. After this step the glycolipids were dissolved with 1 V of acetone. The glycolipids were not needed therefore this fraction was discarded. The phospholipids were collected with 4 V of MeOH. The neutral lipids and phospholipids were evaporated with a rotary evaporator to a small volume.

2.4.3 Mild alkaline hydrolysis (plus methylation):

Carboxyl ester groups are more susceptible for nucleophilic attacks by different ions, like hydroxyl ions, than the phosphate groups. Therefore mild alkaline hydrolysis was used to deacylate the phospholipids. The ester bonds between the glycerol backbone and the fatty acid side chains are thus cleaved. During methylation fatty acid methyl esters, called FAMEs, are formed from the released fatty acids. This methylation is done to obtain substances which can be measured by gas chromatography, because the substances get less polar and more volatile and have a higher thermal stability. For this purpose the samples were methylated and hydrolyzed with a methanolic KOH solution (0.2 M) at 37°C. The pH of the samples was adjusted to 6 with acetic acid (1 M).
After this 10 mL of chloroform and 10 mL of water was added, mixed for 1 min and centrifuged. The lower chloroform phase was removed and passed through a funnel. The funnel was filled with a small amount of fiberglass and sodium sulphate anhydrous powder. Sodium sulphate was used to remove all remained water. The water phase was extracted twice more with 5 mL of chloroform and the chloroform phase was dried with the rotary evaporator to a small volume.

2.4.4 Separation of unsubstituted FAMEs

After the hydrolysis and methylation the unsubstituted FAMEs got separated with NH_2 columns. The columns had a size of 0.5 g/3.5 mL. To condition the columns 1 Volume of a hexane : dichloromethane (DCM) (3:1, v:v) solution was applied. Afterwards samples dissolved in a hexane : DCM (3:1; v:v) solution were applied on the column and was washed out of the column with 1 V of hexane : DCM (3:1; v:v) again. After this step the NLFA fraction did not need further preparation.

2.4.5 Separation of unsubstituted ester linked PLFAs

The PLFAs were then separated into saturated fatty acids (SATFA), monounsaturated fatty acids (MUFA) and polyunsaturated fatty acids (PUFA) using SCX columns impregnated with silver. This separation allows a better analysis of the PLFAs. The different saturation levels lead to different polarity features. The columns had a size of 0.5 g/3 mL. The columns were conditioned with a solution of 0.1 g of silvernitrate in 1.5 mL of acetonitrile, followed by 2 V of acetonitrile, 2 V of acetone and 4 V of DCM. The sample was then applied onto the column

and dissolved in 2 V of DCM : hexane (7:3; v/v) to elute the SATFAs. To obtain the MUFAs 2 V of DCM : acetone (9:1; v/v) was applied to the column. Finally, the PUFAs were eluted with 4 V of acetone : acetonitrile (9:1; v/v).

All samples (NLFA/PLFA) were dried over Nitrogen (N) gas until all liquid was removed, dissolved in 200 µL stock solution with n19:0 in isooctane as internal standard and transferred to 2 mL vials with an inlet. These vials were stored in the freezer (-20°C) until measurement.

For the NLFA, SATFA and MUFA a stock solution concentration of 100 ng/µL was used and for the PUFA a concentration of 50 ng/µL, because PUFAs were expected to appear in a lower concentration.

2.5 Measurement of the samples

2.5.1 Gas chromatograph coupled with flame ionization detector

To quantify the content of PLFAs and NLFAs the samples were measured with a gas chromatograph (GC) coupled to a flame ionization detector (FID). Gas chromatography is a wide used instrumental analysis technique, which offers a high resolution of compound separation in a wide range of components. The separation of components occurs mainly by the differences on their volatility and structural properties.

In the presented thesis a *Hewlett Packard HP 6890* series GC-System coupled with a FID (Agilent Technologies, Palo Alto USA) was used. One Aliquot of each sample was injected in an injector in split mode, where 1:10 of the sample was transferred to the column. Injections were performed at 280°C. The components were vaporized and carried to the column with a Helium flow of 2 mL/min. Here an *Agilent ultra 2* capillary column was used with a length of 45 m. The stationary phase had a film of 0.52 µm and an inner diameter of 0.32 mm. The vaporized analytes interact with the stationary phase on the column. This interactions lead to the separation of different compounds in one sample. The molecules of each compound distribute between the mobile and stationary phase. For every molecule entering the stationary phase, another one leaves the stationary phase to take its place in the mobile phase (Baugh, 1993). Due to different properties of the molecules the distribution in the column differs and a separation of the molecules occurs. The column is placed in an oven which was heated up from 60°C to 270° C with a rate of 2°C/min and this temperature was hold for 6 min. From there the oven was heated up to 320°C with a rate of 30ºC/minute and a final hold time of 3 minutes. The heating process intensifies the separation of the components. The substances are transported to the FID, where the molecules are combusted in a hydrogen flame. During this process ions of the organic compounds were generated. These ions were detected by a collector electrode above the flame and an ion current is measured. For every signal a peak emerges. The peaks were integrated automatically by the *Isodat 2* software. Each sample was measured two times, to minimize analytical faults.

For the quantification a calibration curve was done. For that a stock solution with fatty acid standards (n12:0-n23:0) was prepared and measured in six different concentrations: 1 ng/µL, 5 ng/µL, 10 ng/µL, 25 ng/µL, 50 ng/µL, 100 ng/µL.
The amount of the compounds in each sample was given in ng/µL. This value was converted to nmol $g^{-1}$and mol percentage (mol%) of PLFAs. All converted values of the several samples are found in the Appendix (Table 2a-c and Table 3a-c).

2.5.2 Isotope-ratio mass spectrometer

For the determination of the C isotope ratio a gas chromatograph-combustion-isotope-ratio mass spectrometer system (GC-c-IRMS) was used. The GC conditions (HP5890 GC, Agilent Technologies, Palo Alto USA) were those described above. The GC is connected to an IRMS (Deltaplus XL, Finnigan Mat, Bremen, Germany) via a combustion interface (GC Combustion III Finnigan Mat, Bremen, Germany), a capillary micro-reactor. Here the compounds were converted into simple CO_2 gas by oxidation at 940°C. Formed nitrous gases were reduced at 600°C to elementary N. The CO_2 gas was transported to the IRMS over a valve. The compounds enter the ionization chamber where they were bombarded by electrons with 150 eV. The ions are deflected by a magnet; the radius is depending on their masses. Three masses are detected for carbon measurements: 44 ($^{12}C^{16}O_2$), 45 ($^{13}C^{16}O_2$, $^{12}C^{16}O^{17}O$) and 46 ($^{12}C^{17}O_2$, $^{13}C^{16}O^{17}O$, $^{12}C^{16}O^{18}O$) the ^{17}O and ^{18}O values were corrected automatically by the device software. The ions are detected simultaneously by a universal triple detector. The signals were displayed as peaks. Areas for every mass were integrated automatically by the software *Isodat 2* and the isotope ratio was calculated. This ratio is based on the integration of the masses 13 (^{13}C) and 14 (^{12}C). The ratio is expressed in the $\delta^{13}C$ notation. The ratio was measured against a standard.

$$\delta^{13}\mathrm{C}(‰) = \frac{\left(\mathrm{R}_{\mathrm{sample}} - \mathrm{R}_{\mathrm{standard}}\right)}{\mathrm{R}_{\mathrm{standard}}} \times 1000$$

With $R=^{13}C/^{12}C$. *Vienna Pee Dee Belemnit Standard* (VPDB) serves as the standard.
At the beginning and at the end of every measurement reference gas of known isotopic composition was passes into the system. Gas was measured against the international reference standard. Each sample was measured three times and the mean was built.
The isotope ratios needed to be correct, because of drifting factors. Therefore an offset was determined:

$$o\mathrm{ffset} = \frac{\delta^{13}\mathrm{C}_{\mathrm{meas}} - \delta^{13}\mathrm{C}_{\mathrm{ref}}}{1 + \delta^{13}\mathrm{C}_{\mathrm{meas}}/1000}$$

Where $\delta^{13}C_{meas}$ stands for the isotope value of the measured sample and $\delta^{13}C_{ref}$ stands for the isotope value of reference values of the internal standard n19:0 in every sample. The offset was then added to the value of every compound:

$$\delta^{13}\mathrm{C}_{\mathrm{sample}} = \delta^{13}\mathrm{C}_{\mathrm{meassample}} + \mathrm{offset}$$

During the methylation step an additional C atom was added to each fatty acid molecule. The added C atom affects the $\delta^{13}C$ values of the PLFAs, therefore the $\delta^{13}C$ (-30.01 ‰) of the used methanol was subtracted out from each compound:

$$\delta^{13}\mathrm{C}_{\mathrm{PLFA}} = \frac{(\mathrm{N}_{\mathrm{PLFA}} + 1) \times \delta^{13}\mathrm{C}_{\mathrm{FAME}} - \delta^{13}\mathrm{C}_{\mathrm{MeOH}}}{\mathrm{N}_{\mathrm{PLFA}}}$$

Where N_{PLFA} stands for the number of C atoms, $\delta^{13}\mathrm{C}_{\mathrm{FAME}}$ for the isotope ratio of the measured component, $\delta^{13}\mathrm{C}_{\mathrm{MeOH}}$ stands for the C isotope ratio of the used methanol.
Standard fatty acid nomenclature was used to describe PLFAs. The number before the colon refers to the total number of C atoms. The number after the colon refers to the total number of double bonds in the components and the number after the ω indicates the position of the double bond counted from the aliphatic end. The prefixes “cy”, “Me”,”i” and “a” stand for the cyclopropane groups, methyl groups, and the iso- and anteiso branched molecules.
The net ^{13}C enrichment (^{13}C nmol g^{-1}) of individual PLFAs was calculated by multiplying the concentration of PLFA with the subtracted $\delta^{13}C$ of the unlabeled control samples from the excess $\delta^{13}C$ in labeled samples.

$$\Delta\delta^{13}\mathrm{C}_{\mathrm{PLFA}}(^{13}\mathrm{C\,nmol\,g^{-1}}) = (\delta^{13}\mathrm{C}_{\mathrm{labeled}} - \delta^{13}\mathrm{C}_{\mathrm{unlabeled}}) \times \mathrm{conc}_{\mathrm{PLFA}}$$

All measured values after the corrections and the ^{13}C enrichment values are found in the Appendix (Table 4a-c and Table 5a-b).

2.6 Statistical analysis

PLFA compositions of the samples were analyzed using CANOCO software (version 5.0, Microcomputer Power, Inc., Ithaca, NY). The concentration (expressed as mol%) of individual PLFA were subjected to principal component analysis (PCA) to elucidate variations and a redundancy analysis (RDA) was performed. PCA was used to extract the major patterns from the variation in PLFA data. The RDA was used to test the time dependency of the PLFA composition. The time component was tested for significant contribution. Significance for the data are reported at the $p<0.05$ level.
For correlation matrix and outlier test the program R 3.0.1 (The R Foundation Statistical Computing, 2013) was used.

3 Results

3.1 Biomarkers

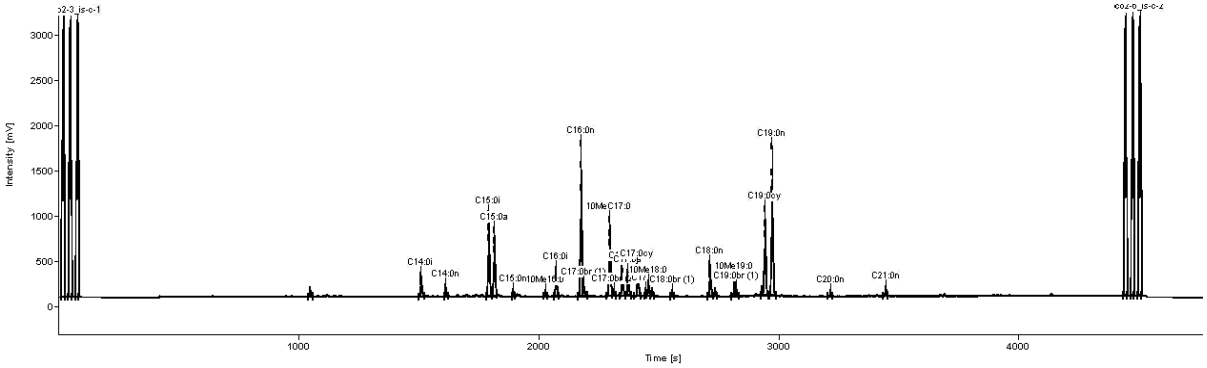

Figure 1: GC-IRMS chromatogram of sample T1 A. An example of a GC-c-IRMS chromatogram of PLFAs extracted from sample T1 A. Shown here is the SATFA fraction. Plotted is the intensity (mV) against the retention time (seconds.) The first and last three peaks are the reference gas peaks.

Chromatograms of PLFAs are the basis for sample analysis (Figure 1). The compounds in the different fractions get separated and every biomarker emerges as single peak. Each substance has a specific retention time under specific chromatography conditions. The separated components were identified by comparing their retention times and elution patterns with that obtained from previous studies at the MPI of biogeochemistry, Jena and from standard runs. 32 PLFA peaks were detected in the samples. For analysis only PLFAs with an abundance greater than 1 mol% of total PLFAs were chosen (excluded were 19:0br and 17:1 because of their non-specificity). In total 18 components were selected for ^{13}C analysis because of their use as specific microbial biomarkers (Table 2). These chosen PLFAs represent 88.16 ± 0.91 % of the total PLFA concentration. From the NLFA fraction only 16:1ω5 was used for analysis.

Table 2: Characteristic fatty acid lipids as indicators for different organism sources.

Indicator	Source	Reference
i14:0, a15:0, i15:0, i16:0, a17:0, i17:0	Gram-positive bacteria	(Frostegard and Baath, 1996, Zelles, 1997)
16:1ω7, 18:1ω7, 19:0cy, 17:0cy, 16:1ω9, 18:1ω5	Gram-negative bacteria	(Frostegard and Baath, 1996, Zelles, 1997, Zou et al., 2013)
18:1ω9, 18:2ω6	fungi	(Frostegard and Baath, 1996)
16:1ω5 (NLFA)	AMF	(Olsson et al., 1995)
16:1ω5 (PLFA)	Bacteria and AMF	(Olsson et al., 1995)
10Me17:0	Actinomycetes	(Zelles, 1999)
n16:0	community	(Denef et al., 2009)
n18:0	general	(Jin and Evans, 2010)

3.2 Soil community composition

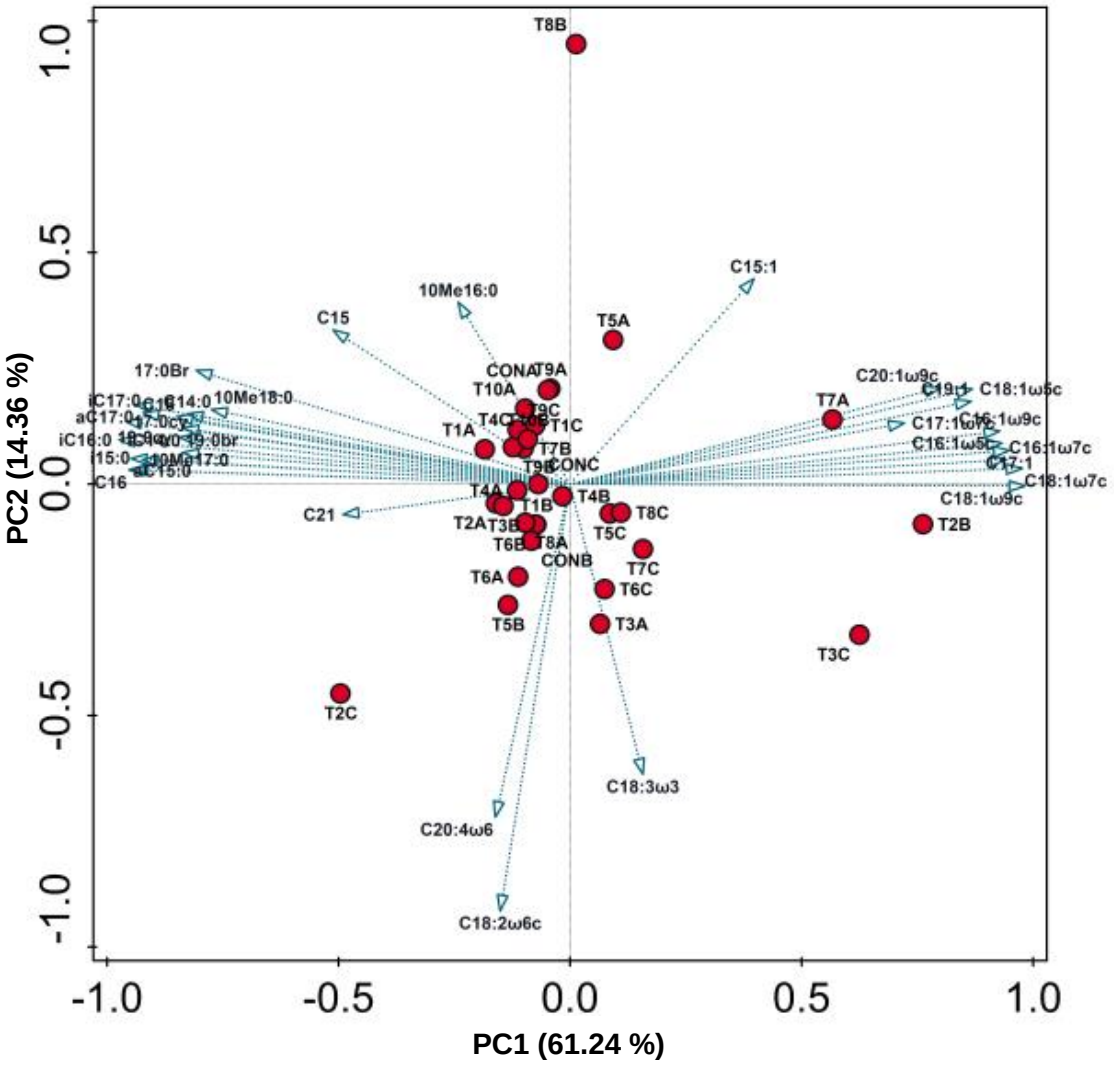

Figure 2: PCA of the PLFA composition from all samples. Principal component analysis of soil microbial community generated by GC-FID analysis of all samples analyzed (red circles). Used is mol% of the detected compounds. PC1 explains 61.24 % of the total variation and PC2 14.36 %.

The PCA of soil microbial community off all samples analyzed summarized the patterns of species composition variation across samples. 61.24 % of the total variation was explained by the first principal component PC1. PC2 explained 14.36 % of the variation (Figure 2). The correlation between substances from one fraction (e.g. SATFA) was positive, whereas components from different fractions were negatively correlated to each other. Samples were found at the intersection of both axes, except for some (T2B, T2C, T3C, T7A and T8B). These differences in samples can be explained by methodical or analytical faults. The PCA of PLFA components showed no variations in the different samples, which was as expected because there was no different treatment of the pots. Time was not a significant factor for

changes (p=0.086), verified with a redundancy analysis (RDA). Therefore, the microbial community did not change and was in steady state during the entire experimental time.

Table 3: Concentration of the total, bacterial* and fungal biomass in the soil samples (nmol g^{-1}).**

	T1A	T1B	T1C	T2A	T2B	T2C	T3A	T3B	T3C	T4A	T4B	T4C
total	39.13	33.00	27.97	24.08	34.26	34.41	25.83	48.30	50.20	69.01	54.29	70.46
bacteria	26.01	21.11	18.00	15.59	21.52	21.97	16.57	30.95	31.46	44.35	34.97	45.28
fungi	0.62	0.63	0.40	0.39	0.41	0.83	0.55	0.81	1.17	1.18	0.87	1.04
	T5A	**T5B**	**T5C**	**T6A**	**T6B**	**T6C**	**T7A**	**T7B**	**T7C**	**T8A**	**T8B**	**T8C**
total	44.26	55.43	48.23	44.07	77.92	41.39	59.43	38.97	37.05	43.96	54.54	48.57
bacteria	28.72	35.63	30.87	28.29	49.91	26.32	37.55	24.71	23.62	28.31	35.41	30.91
fungi	0.39	1.15	0.91	0.91	1.52	0.85	0.72	0.55	0.67	0.77	-	0.90
	T9A	**T9B**	**T9C**	**T10A**	**T10B**	**CON A**	**CON B**	**CON C**				
total	38.82	42.53	35.66	43.02	50.97	38.36	40.63	31.59				
bacteria	24.71	27.26	22.86	27.47	32.34	24.60	25.87	20.09				
fungi	0.56	0.70	0.52	0.57	0.86	0.45	0.86	0.72				

* For total bacterial biomass calculation PLFAs of Gram-positive bacterial and Gram-negative bacterial compounds were used (i14:0, a15:0, i15:0, i16:0, a17:0, i17:0, 16:1ω5, 16:1ω7, 16:1ω9, 18:1ω5, 18:1ω7, 19:0cy, 17:0cy, 10Me17:0)

** For total fungal biomass PLFA 18:2ω6 was used.

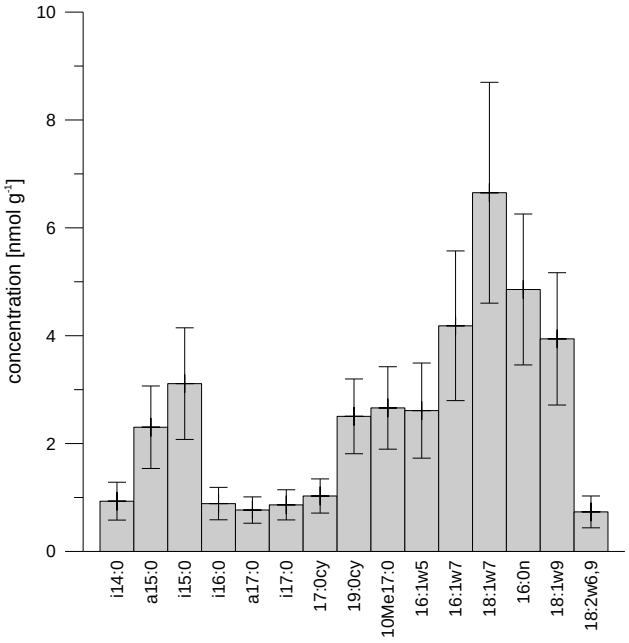

Figure 3: Mean concentration of analyzed PLFAs. Concentration in nmol g-1 of the 15 important PLFAs in the samples. The mean of all samples was used to display the concentration. The error bars show the standard deviations of the differences between the analyzed samples (n=32).

The sum of the total extractable PLFAs from each soil sample has previously been shown to be proportional to other microbial biomass measures (Fritze et al., 2000, Fierer et al., 2003). Most prevalent phosphor lipids in the soil samples were SATFAs and MUFAs. Both these fractions amounted for 97.5 ± 0.01 mol% of all detected PLFAs in the samples; the rest were PUFAs. The total amount of PLFAs varied between 24.08 and 77.92 nmol g^{-1} in the different samples (Table 3). The sum of i14:0, a15:0, i15:0, i16:0, a17:0, i17:0, 16:1ω5, 16:1ω7, 16:1ω9, 18:1ω5, 18:1ω7, 19:0cy, 17:0cy and 10Me17:0 was used as bacterial biomass and varied between 15.59 and 49.91 nmol g^{-1}. In total they comprised 66.50 ± 0.69 mol% of the total amount of PLFA. 18:2ω6,9 was used as a measure of the fungal biomass and had the lowest concentration with values between 0.39 and 1.52 nmol g^{-1}.

Statistically significant differences in the communities between the growing pots were not found; therefore the mean concentration of all samples was calculated to show the variation in the concentration of the different biomarkers (Figure 3). The most abundant component in all pots was 18:1w7 with concentration between 3.33 and 11.50 nmol g^{-1}, followed by the general biomarker n16:0 (2.45- 8.52 nmol g^{-1}). The 16:1ω7 marker also had a high concentration in the analyzed soil samples (1.87- 7.46 nmol g^{-1}). The most abundant Gram-positive bacterial biomarker was i15:0. The fungal biomarker 18:2ω6 was the least abundant.

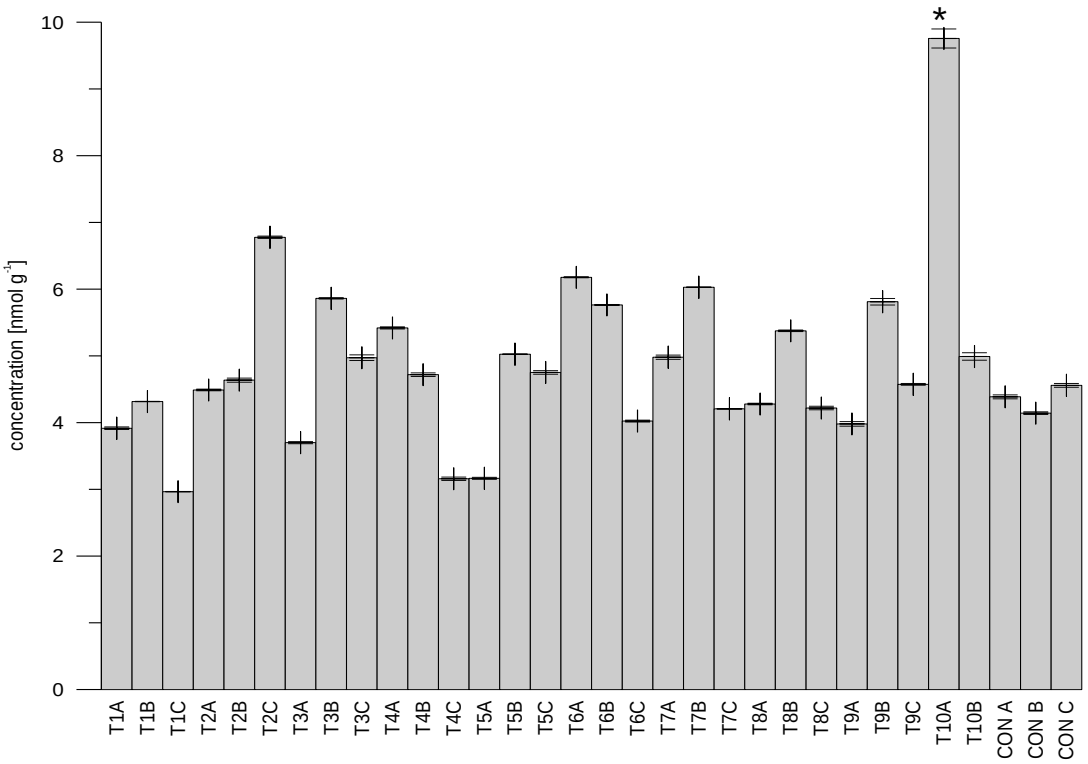

Figure 4: NLFA 16:1ω5 concentration in the samples. Concentration in nmol g¹ of the NLFA component 16:1ω5 in all samples obtained from GC-FID measurement. The error bars show the standard deviation between the two measurement runs (n=2).

The 16:1ω5 NLFA concentration was significantly higher in sample T10A (9.76 nmol g^{-1}), whereas the amount in other samples was lower (minimum of 2.96 nmol g^{-1} in sample T1C and maximum of 6.77 nmol g^{-1} in T2 C) (Figure 4). Sample T10 A was identified as an outlier with a descriptive statistics (boxplot diagram Figue A1). The standard deviation between the replicated runs for the NLFA fraction varied between 0.01 and 0.14 ‰.

3.3 Lipid incorporation of photosynthetically fixed ^{13}C

Pulse labelling resulted in significantly higher ^{13}C enrichment of several PLFAs relative to the three unlabeled control. The $\delta^{13}C$ value of biomarkers in the control soil varied from -31.62 ‰ in 19:0cy and -25.72 ‰ in a17:0. The standard deviation between the different control soil replicates varied between 0.22 and 1.12 ‰ in the SATFA and MUFA fraction. The standard

deviation for the PUFA compound 18:2ω6 was 3.92 ‰, higher than usual due to the small amount detected in the samples. The standard deviation of the NLFA compound in the control pots was 0.22 ‰. Incorporation of ^{13}C varied temporally for the different microbial biomarkers.

3.4 Fungal lipid biomarkers

3.4.1 Saprophytic and general fungi

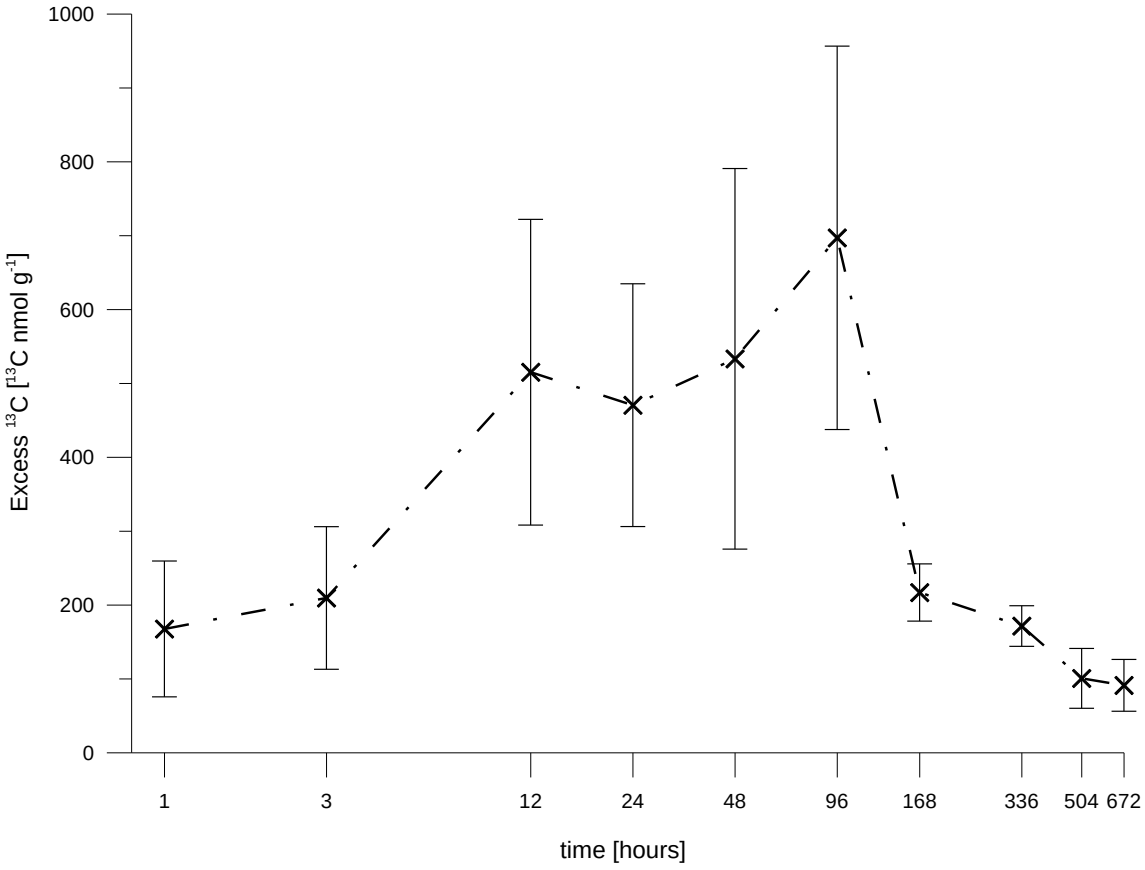

Figure 5: Saprophytic fungal biomarker ^{13}C enrichment. ^{13}C excess in ^{13}C nmol g^{-1} of the saprophytic fungal biomarker 18:2ω6,9 over the entire sampling period. The x-axis shows the sampling time points in hours and is based on a $\log_{10}$ scale. The error bars show the standard deviations between the three replicates at each time point.

The 18:2ω6,9 component had an enrichment of 167.55 ± 91.96 ^{13}C nmol g^{-1} immediately after labeling (Figure 5). The value increased up to the sixth time point (96h after pulse labeling) to a maximum of 697.02 ± 259.54 ^{13}C nmol g^{-1}. After 96 hours the enrichment decreased until four weeks after the labeling. After 336 hours or 2 weeks the enrichment returned to the initial value. The decrease in enrichment was slower than the rise at the start. A minimum of 91.23 ± 35.11^{13}C nmol g^{-1} was reached four weeks after labeling, still showing relative high enrichment compared to the unlabeled control samples.

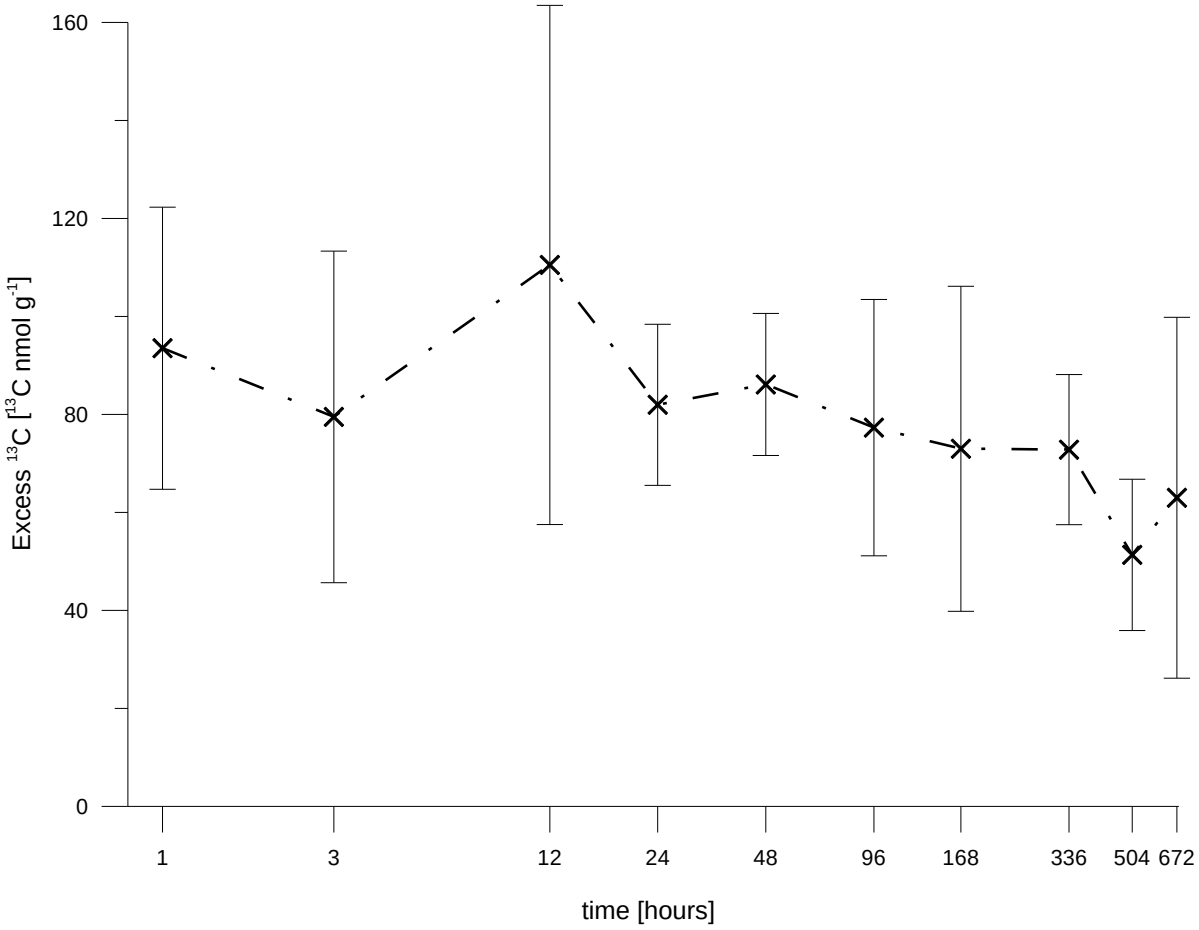

Figure 6: General fungal biomarker ^{13}C enrichment. ^{13}C excess in ^{13}C nmol g^{-1} of the general fungal biomarker 18:1ω9 over the entire sampling period. The x-axis shows the sampling time points in hours and is based on a $\log_{10}$ scale. The error bars show the standard deviations between the three replicates at each time point.

The general biomarker for fungi 18:1ω9 exhibited a small decrease of the enrichment towards the end of the sampling period (Figure 6). The incorporation was relatively stable over the experimental period and varied from 51.33 ± 15.45 ^{13}C nmol g^{-1} at T9 to 110.51 ± 52.99 ^{13}C nmol g^{-1} at T3. The incorporation of labelled carbon started immediately after labeling with 93.51 ± 28.79 ^{13}C nmol g^{-1}.

3.4.2 Arbuscular mycorrhiza fungi

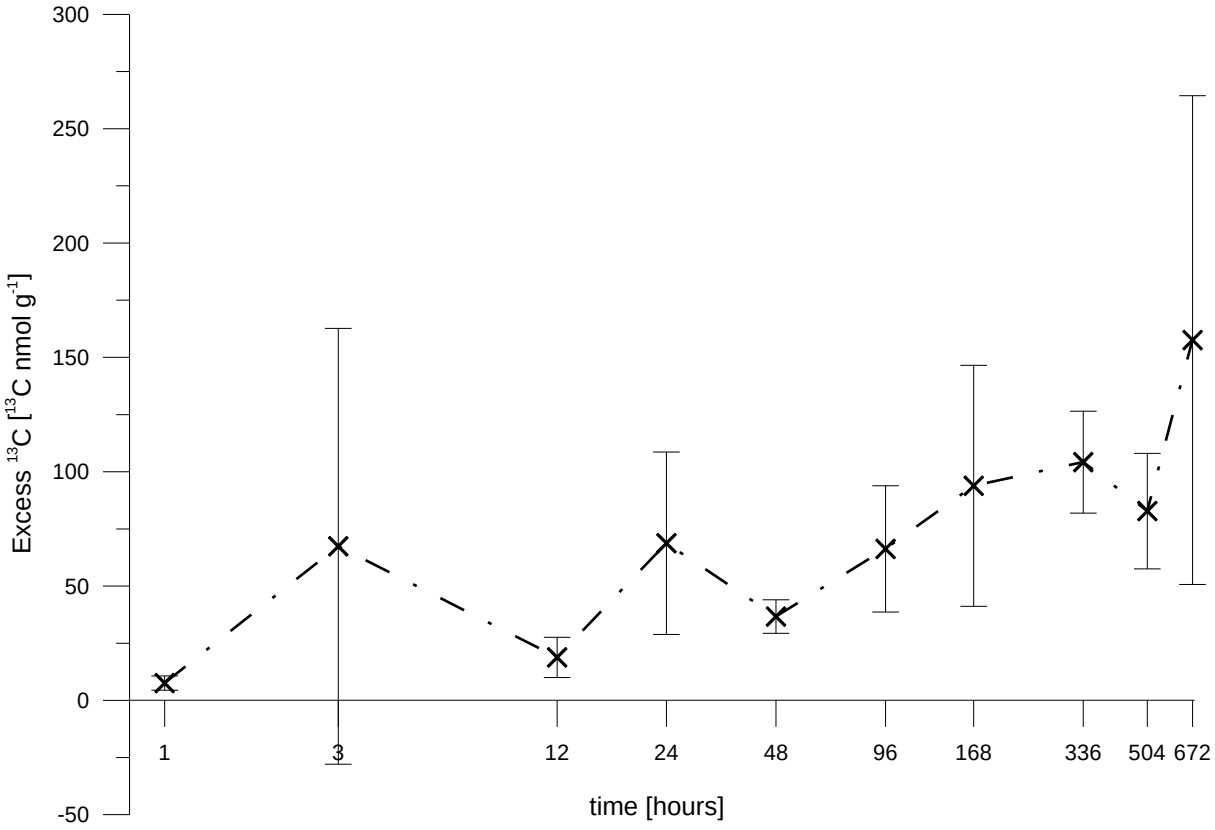

Figure 7: Arbuscular mycorrhizal fungi PLFA biomarker ^{13}C enrichment. ^{13}C excess in ^{13}C nmol g^{-1} of the AM fungi PLFA biomarker 16:1ω5 over the entire sampling period. The x-axis shows the sampling time points in hours and is based on a $\log_{10}$ scale. The error bars show the standard deviations between the three replicates at each time point.

The AMF PLFA marker 16:1ω5 showed an increasing trend in ^{13}C enrichment until the end of the experiment (Figure 7). It showed a fluctuating but increasing enrichment starting with 7.54 ± 3.15 ^{13}C nmol g^{-1}. The highest enrichment of 157.56 ± 106.90 ^{13}C nmol g^{-1} was seen at the last time point. The standard deviation of T2 and T10 were relatively high with values of 95.31 and 106.90 ^{13}C nmol g^{-1} respectively.

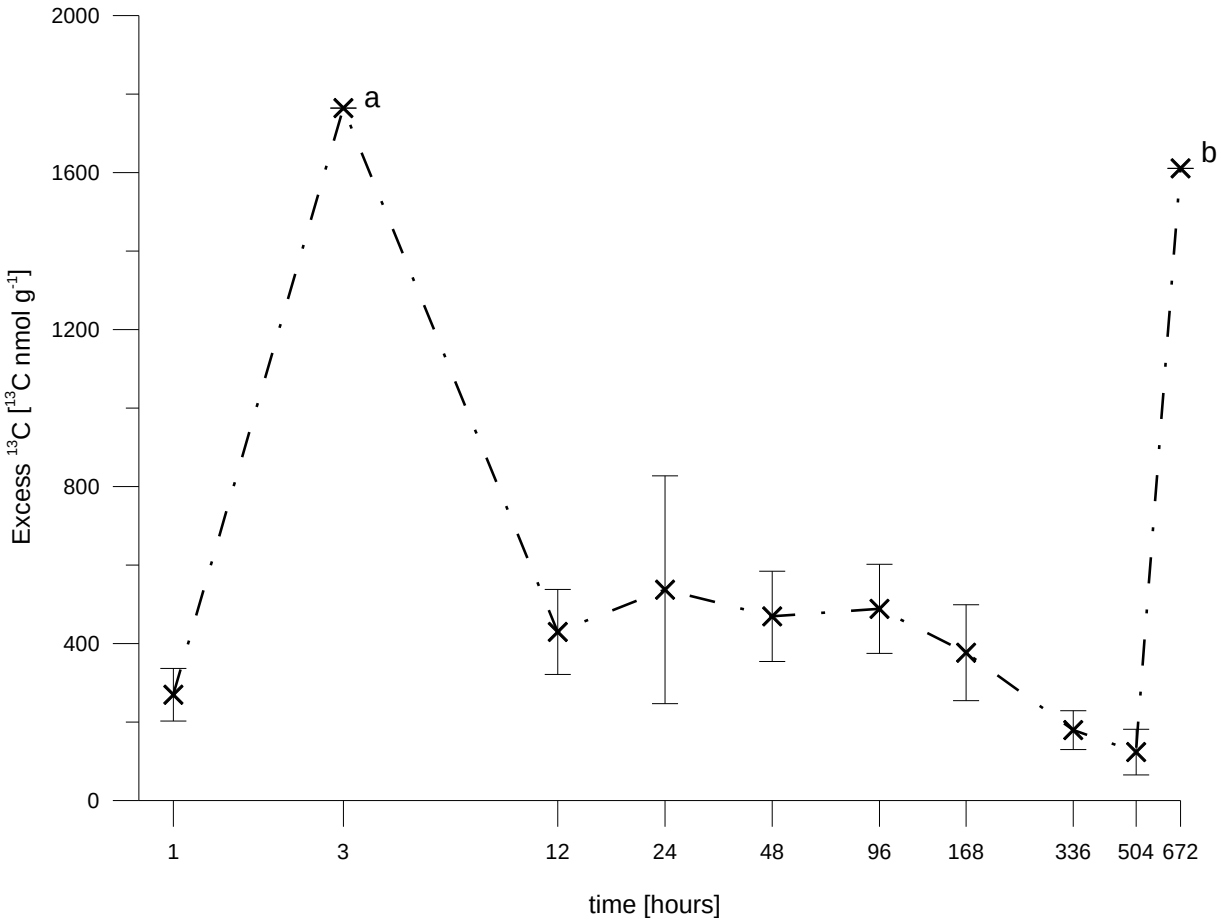

Figure 8: Arbuscular mycorrhiza fungi NLFA biomarker ^{13}C enrichment. ^{13}C excess in ^{13}C nmol g^{-1} of the AM fungi NLFA biomarker 16:1ω5 over the entire sampling period. The x-axis shows the sampling time points in hours and is based on a $\log_{10}$ scale. The error bars show the standard deviations between the three replicates at each time point. Standard deviation for (a) T2 (2291.87 ^{13}C nmol g^{-1}) and (b) T10 (1998.53^{13}C nmol g^{-1}) were excluded from the diagram because of the high values.

The AMF NLFA marker showed an increasing enrichment until 24 hours after labeling with the highest enrichment of 1764.34 ± 2291.87 ^{13}C nmol g^{-1} at the second time point (Figure 8). From this point on the enrichment was relatively constant between 376.78 ± 122.09 ^{13}C nmol g^{-1} and 488.43 ± 113.57 ^{13}C nmol g^{-1} until one week after the labeling. Then the enrichment started decreasing up to 123.56 ± 58.16 ^{13}C nmol g^{-1} at T9. The enrichment after 4 weeks was high (1610.83 ± 1998.53 ^{13}C nmol g^{-1}), due to the high enrichment in sample T10A. A decreasing trend is clearly visible from the beginning to the end of the experiment. The standard deviation of T2 (2291.87 ^{13}C nmol g^{-1}) and T10 (1998.53 ^{13}C nmol g^{-1}) were very high in contrast to the standard deviation at other time points which varied between 49.56 and 290.14 ^{13}C nmol g^{-1}.

3.5 Bacterial lipid biomarkers

3.5.1 Gram-positive bacteria

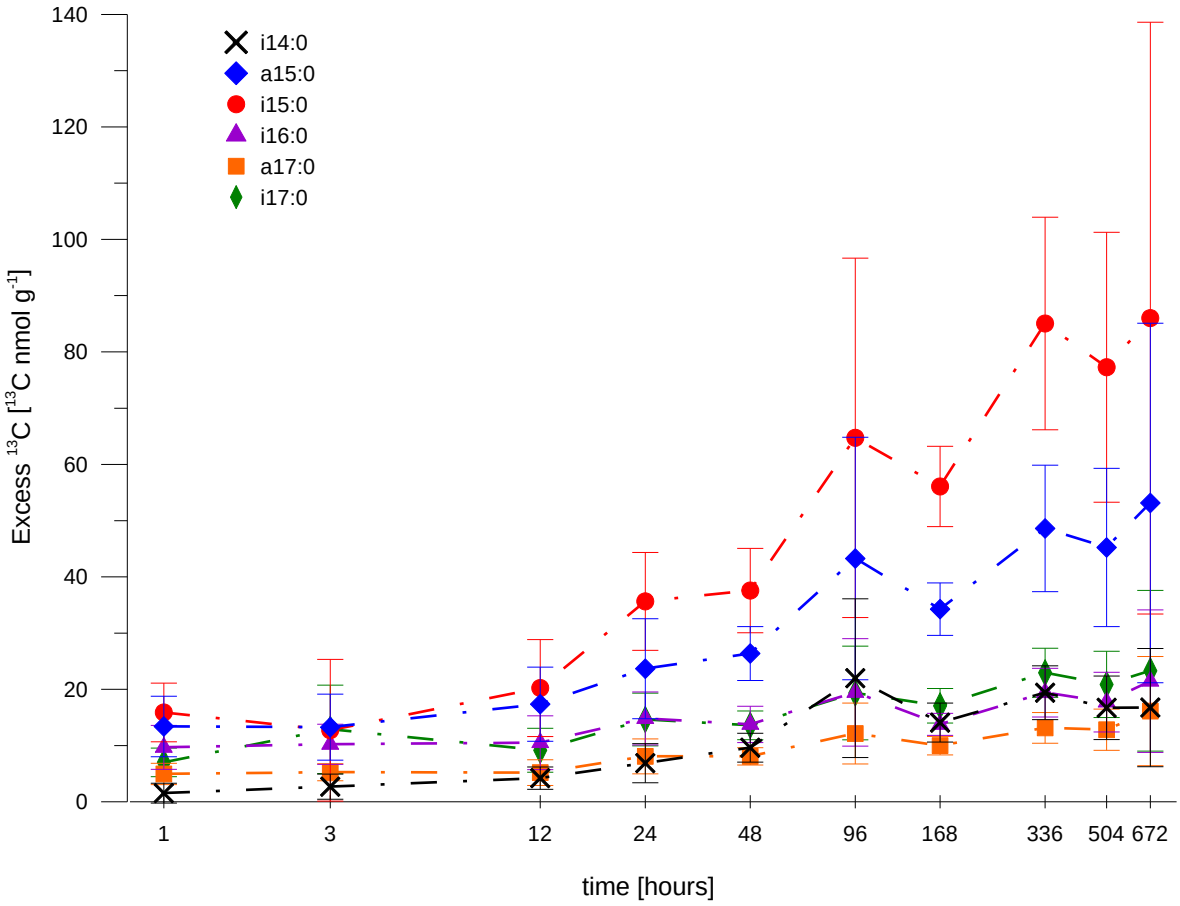

Figure 9: Gram-positive bacterial biomarkers ^{13}C enrichment. ^{13}C excess in ^{13}C nmol g^{-1} of the Gram-positive bacterial biomarkers over the entire sampling period. The x-axis shows the sampling time points in hours and is based on a $\log_{10}$ scale. The error bars show the standard deviations between the three replicates at each time point.

The Gram-positive lipid biomarkers (i14:0, a15:0, i15:0, i16:0, a17:0 and i17:0) showed a similar course of ^{13}C incorporation to each other (Figure 9). The enrichment increased over the time. The first time point (immediately after labeling) had the lowest values in almost all components. The lowest enrichment at T1 had i14:0 with 1.53 ± 1.76 ^{13}C nmol g^{-1} and the highest enrichment at T1 had i15:0 with 15.88 ± 5.22 ^{13}C nmol g^{-1}. The enrichment was fluctuating rising until the end of the experimental time. The enrichment at T10 varied between 16.12 ± 9.70 ^{13}C nmol g^{-1} in a17:0 and 86.01 ± 52.62 ^{13}C nmol g^{-1} in i15:0.

3.5.2 Gram-negative bacteria

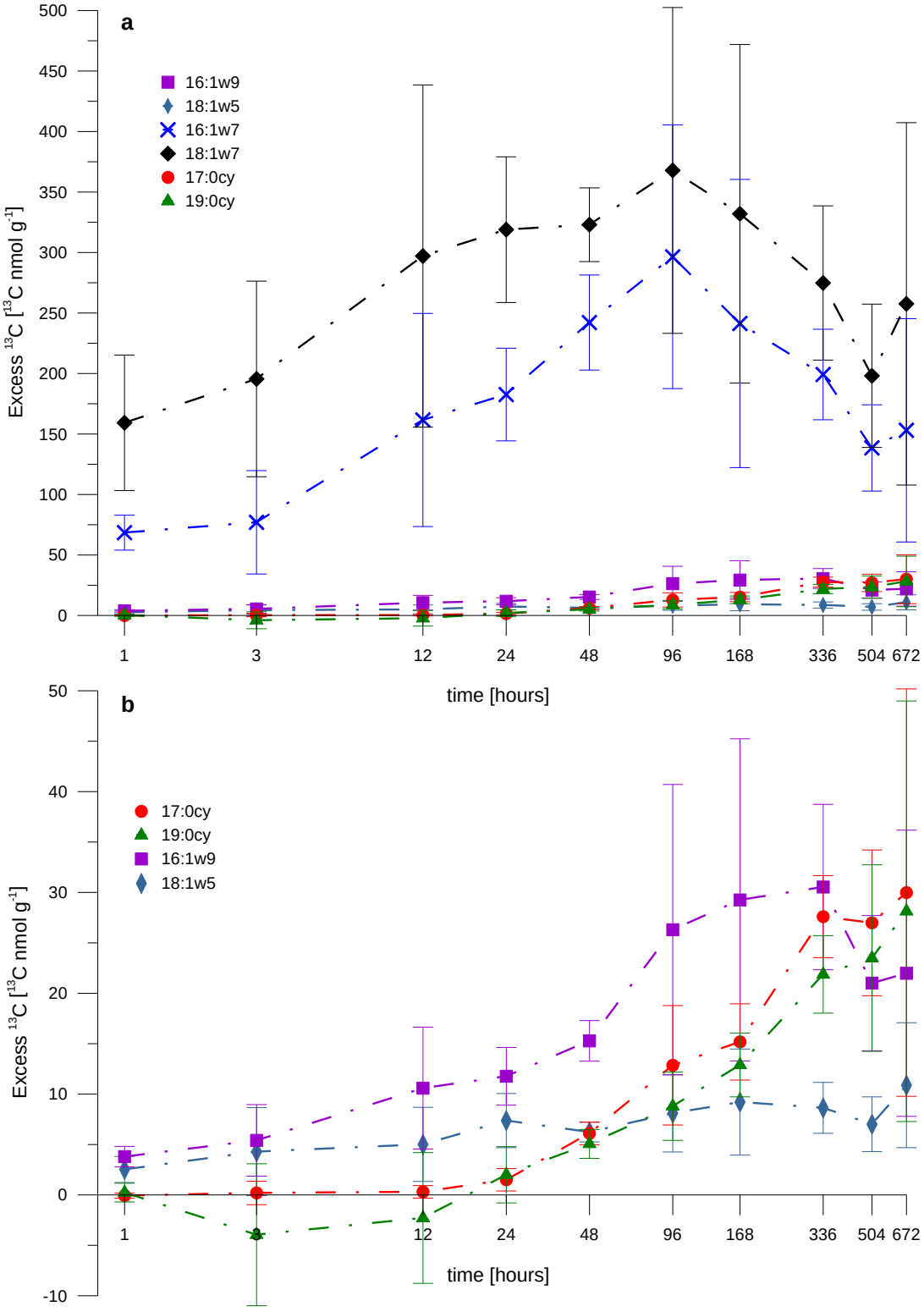

Figure 10: Gram-negative bacterial biomarkers ^{13}C enrichment. (a) ^{13}C excess in ^{13}C nmol g^{-1} of all Gram-negative bacterial biomarker compounds (16:1ω7, 18:1ω7, 16:1ω9, 18:1ω5 17:0cy and 19:0cy) over the entire sampling period, (b) shows the cyclopropyl components (17:0cy and 19:0cy) and 16:1ω9 and 18:1ω5 in detail. The x-axes show the sampling time points in hours and are based on a log$_{10}$ scale. The error bars display the standard deviations between the three replicates at each time point.

The Gram-negative biomarkers differed between the classes. The saturated fatty acids 17:0cy and 19:0cy displayed the same trend, the monounsaturated markers 16:1ω5, 16:1ω7, 18:1ω7 and 18:1ω9 differed from the cyclopropyl-component (Figure 10a). But also 16:1ω7 and 18:1ω7 showed a different pattern to 16:1ω5 and 18:1ω9. 16:1ω5 and 18:1ω9 have a small enrichment around the values of the cyclopropyl-components. Both markers showed small ^{13}C enrichment already at the beginning between 2.53 ± 1.30 and 3.80 ± 1.02 ^{13}C nmol g^{-1}. 16:1ω9 displayed a rising trend to the maximum of 30.54 ± 8.21 ^{13}C nmol g^{-1} at time point 8. After that, the enrichment was decreasing. In contrast the marker 18:1ω9 exhibited a slight decreasing but is more or less stable over the sampling period with the maximum of 10.88 ± 6.19 ^{13}C nmol g^{-1} at the last sampling point. The components 16:1ω7 and 18:1ω7 started already with a label of 68.48 ± 14.46 ^{13}C nmol g^{-1} and 159.27 ± 56.02 ^{13}C nmol g^{-1} (Figure 10a). T1 had the lowest incorporation. The enrichment of 16:1ω7 was increasing until 96 hours (T6) after the labeling with a maximum of 296.46 ± 108.97 ^{13}C nmol g^{-1}. From T6 on the enrichment was decreasing to 138.47 ± 35.67 ^{13}C nmol g^{-1} three weeks after the experiment. At the last time point an increasing was seen again. The enrichment of 18:1ω7 showed a similar course but with a higher enrichment. ^{13}C enrichment was rising until the maximum of 367.85 ± 134.67 ^{13}C nmol g^{-1} at T6. After the sixth time point the values were sinking to the minimum of 198.10 ± 59.21 ^{13}C nmol g^{-1} at T9 and T10 had a slightly increasing again. These components showed a fast incorporation, with a sharp decreasing of the enrichment. In contrast, the components 17:0cy and 19:0cy displayed a rising trend from the first time point to the end of the experiment (Figure 10b). These two components had a very slow and low incorporation of the labeled carbon. The values from T1 to T3 of 17:0cy were between -0.07 ± 0.26 ^{13}C nmol g^{-1} and 0.31 ± 0.63 ^{13}C nmol g^{-1} and of 19:0cy between 0.28 and -2.64 ^{13}C nmol g^{-1} and 0.23 ± 0.93 ^{13}C nmol g^{-1}. This showed no incorporation of ^{13}C labeled carbon in these biomarkers in the first three time points. The first incorporation was seen in time point 4, after 24 hours and it increased until the maximum of 29.98 ± 20.21 ^{13}C nmol g^{-1} in 17:0cy and 28.14 ± 20.85 ^{13}C nmol g^{-1} in 19:0cy.

3.5.3 Actinomycetes

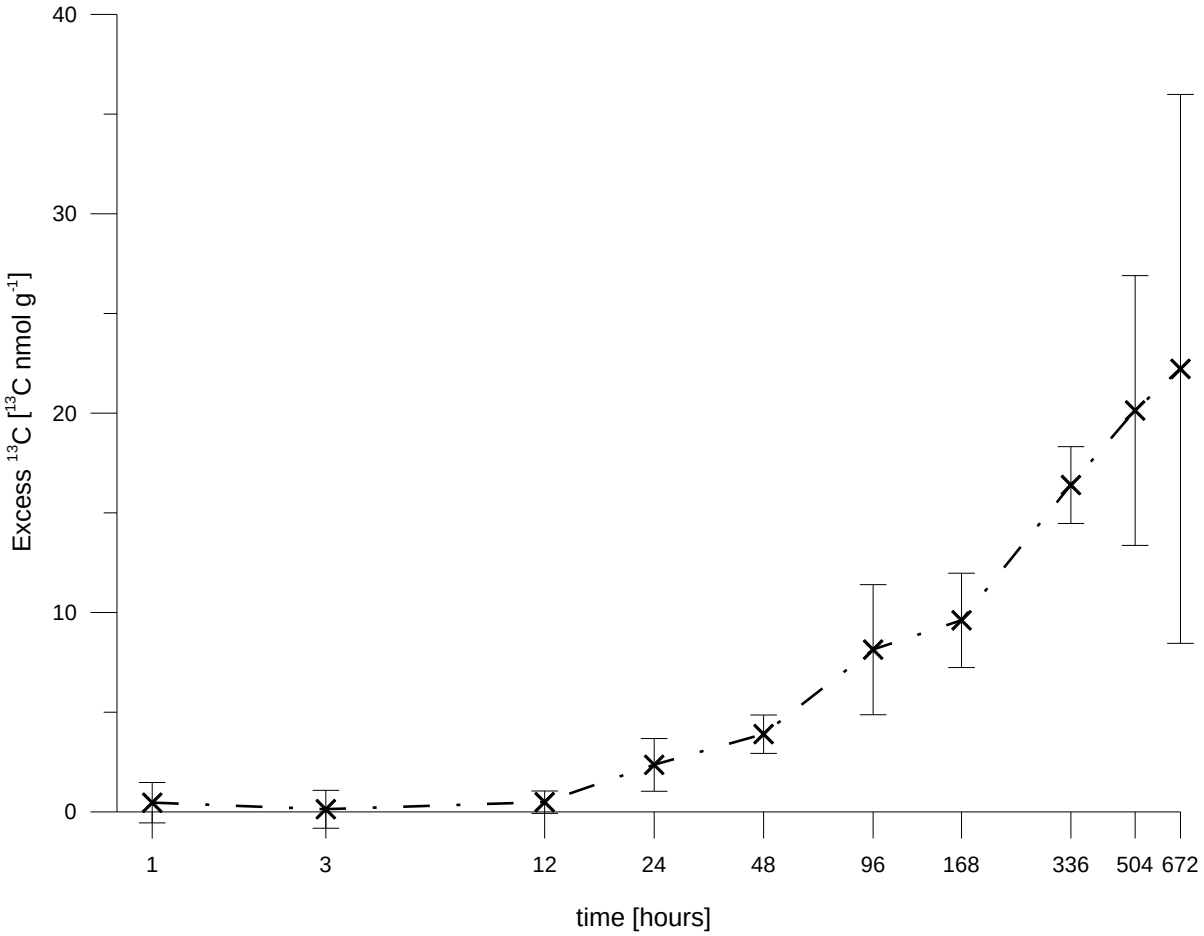

Figure 11: Actinomycetes biomarker ^{13}C enrichment. ^{13}C excess in ^{13}C nmol g^{-1} of the Actinomycetes biomarker 10Me17:0 over the entire sampling period. The x-axis shows the sampling time points in hours and is based on a $\log_{10}$ scale. The error bars show the standard deviations between the three replicates at each time point.

The biomarker for Actinomycetes 10Me17:0 had a very low enrichment over the whole sampling time (Figure 11). An increasing of the enrichment was seen from T1 to three weeks after the labeling. At the beginning there was almost no enrichment with 0.46 ± 1.01 ^{13}C nmol g^{-1} and it rose strongly to the maximum 22.22 ± 13.77 ^{13}C nmol g^{-1} at T10. In total the enrichment of this biomarker was very low. It showed a slow enrichment over the whole experimental time.

3.6 General biomarkers

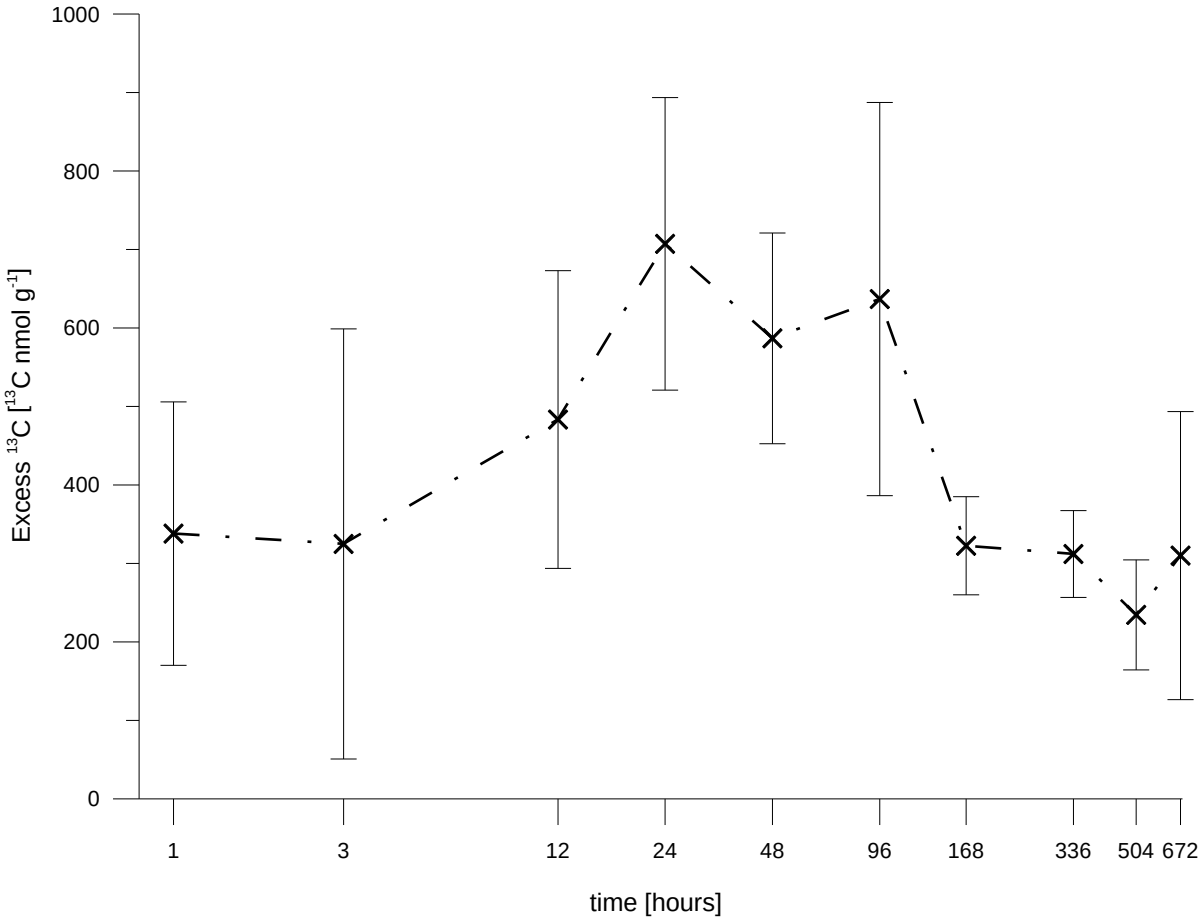

Figure 12: Communitiy biomarker ^{13}C enrichment. ^{13}C excess in ^{13}C nmol g^{-1} of the general biomarker n16:0 over the entire sampling period. The x-axis shows the sampling time points in hours and is based on a $\log_{10}$ scale. The error bars show the standard deviations between the three replicates at each time point.

The general biomarker n16:0 had an enrichment of 338.03 ± 167.82 ^{13}C nmol g^{-1} at the first time point (Figure 12). Then it was rising until 24 hours after the labeling to the maximum of 707.13 ± 186.35 ^{13}C nmol g^{-1}. From there a fluctuating decrease was seen until the minimum of 234.46 ± 70.07 ^{13}C nmol g^{-1} at T9. T10 had a slightly higher amount then T9. At T7 (168 h after labeling) the value from T1 was reached again. This biomarker showed the highest enrichment of all biomarkers. At the beginning the enrichment rose fast and the decreasing of ^{13}C enrichment was relatively slow to that. At the end of the experiment still a lot of label was left in the biomarker.

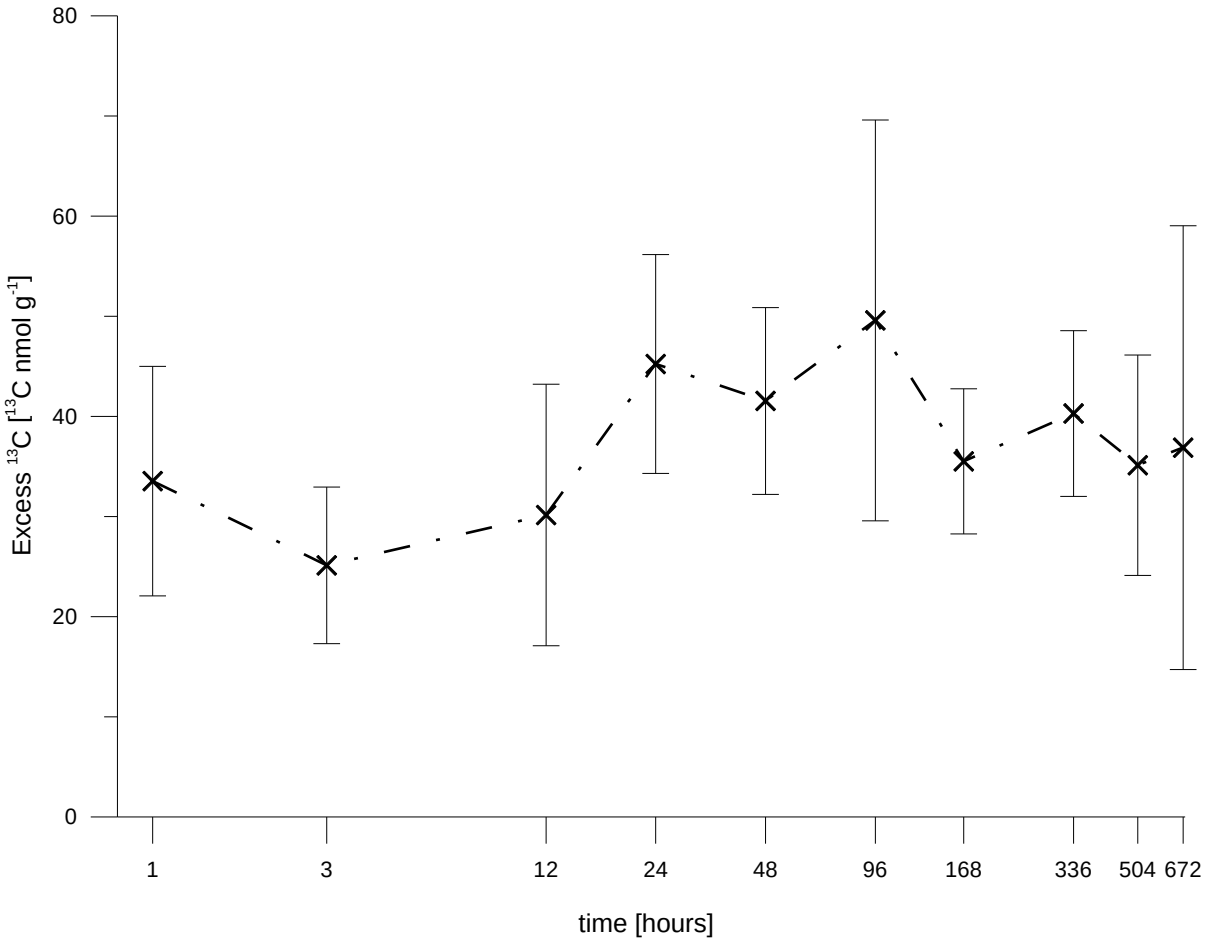

Figure 13: Nonspecific biomarker ^{13}C enrichment. ^{13}C excess in ^{13}C nmol g^{-1} of the nonspecific biomarker n18:0 over the entire sampling period. The x-axis shows the sampling time points in hours and is based on a $\log_{10}$ scale. The error bars show the standard deviations between the three replicates at each time point.

The n18:0 unspecific biomarker showed an enrichment of 33.54 ± 11.46 ^{13}C nmol g^{-1} already at the first sampling point (Figure 13). It had a scattering rising trend until the maximum of 49.58 ± 20.01 ^{13}C nmol g^{-1} 96 hours after the labeling. Then it was decreasing sharply to time point 7 and the values fluctuated until the tenth time point between 35.13 ± 7.25 and 40.29 ± 8.27 ^{13}C nmol g^{-1}.

4 Discussion

4.1 Data review

Variance in measurements of control samples with no isotope enrichment gives a good indication of replicated sample processing and extraction procedure. The low standard deviation of isotope values obtained from three independent replicates of control pots suggests that the extraction procedure was highly reproducible. The standard deviation of isotope values was higher for extracts from the experimental pots because the enrichment in the lipids extracted from these soils was higher. In addition, the differences between the independent experimental replicates in ^{13}C labelling of plants and the subsequent root exudates also lead to higher variance. This was observed in all sampling points after the ^{13}C pulse was applied because of dynamic plant-soil carbon flux.

The highest label was found in the 16:1ω5 NLFA marker of the T2 and T10 triplicates. The PLFA 16:1ω5 also displayed higher enrichment in these samples. A significantly higher labeling of AMF marker was seen at both these time points. This could be because the AMF symbiosis was better established in these pots and therefore more carbon was transferred from roots to the symbiont. Because of this significantly higher enrichment in these soil samples, the two values were excluded from the discussion.

4.2 Microbial community composition

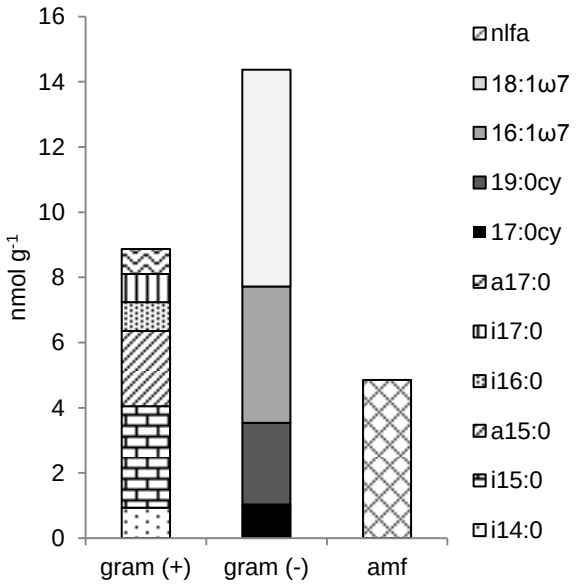

Figure 14: Distribution of the concentration of different microbial groups. The diagram shows the composition of the microbial communities of Gram-positive bacteria, Gram-negative bacteria and AMF in terms of the average concentration from all samples in nmol g^{-1}.

The PCA analyses showed that the pattern of PLFA composition from the different soil samples did not change over the experimental period, suggesting no temporal change in the microbial community structure. These stable conditions were intended and obtained through treatment similarities. Gram-negative bacteria were the most common bacteria in the soil community from the analyzed samples, higher than the Gram-positive bacteria (Figure 14). Gram-negative bacteria are known to be the main inhabitants in rhizosphere soil (Alexander, 1977) and are characterized by a high reproductive rate with high activity under conditions of sufficient

nutrient supply (Soderberg et al., 2004). Gram-positive bacteria are known to play a more important role in bulk soil (Lu et al., 2007). Fungal biomass was very small in the analyzed soil samples; the saprophytic fungal (SF) biomarker 18:2ω6,9 was less abundant in all samples. The ratio of fungal and bacterial biomass, measured as the ratio of 18:2ω6,9 and PLFA bacteria, was around 0.03, which displayed the dominant occurrence of bacteria in the soil samples. In contrast to the SF, the AMF NLFA marker 16:1ω5 had a higher occurrence, suggesting a dominant role of Arbuscular mycorrhizal fungi in plant-soil systems with AMF symbiosis.

4.3 Pool origin of the biomarkers

Table 4: Correlation matrix of the ^{13}C enrichment values of the different analyzed microbial biomarkers.

	i15	19cy	16:1ω7	18:1ω7	Actino	n16:0	18:1ω9	18:2ω6	16ω5P	nlfa	18:1ω5	16:1ω9
19:0cy	0.96											
16:1ω7	0.43	0.22										
18:1ω7	0.23	0.01	0.93									
Actino	0.95	0.99	0.17	-0.03								
n16:0	-0.28	-0.47	0.53	0.69	-0.50							
18:1ω9	-0.77	-0.80	-0.09	0.14	-0.83	0.44						
18:2ω6,9	-0.29	-0.51	0.63	0.73	-0.51	0.90	0.53					
16:1ω5P	0.93	0.89	0.46	0.34	0.86	-0.19	-0.72	-0.29				
nlfa	-0.53	-0.70	0.47	0.67	-0.72	0.90	0.59	0.88	-0.38			
18:1ω5	0.85	0.78	0.59	0.54	0.76	-0.03	-0.61	-0.10	0.94	-0.18		
16:1ω9	0.87	0.75	0.71	0.53	0.72	-0.14	-0.56	-0.05	0.87	-0.23	0.84	
n18:0	0.45	0.25	0.76	0.68	0.20	0.66	-0.19	0.55	0.46	0.38	0.48	0.50

Incorporation of ^{13}C varied temporally and quantitatively for the different microbial markers. The source of different lipids has not been totally clarified yet with some biomarkers found in several organism pools (Frostegård et al., 2011). It may be difficult to interpret the lipid profiles of soil communities, since many fatty acid are common in different microorganisms (Zelles, 1999). Prior to use of a particular marker for specific organism groups it is recommended to group similar biomarkers by means of statistical analysis (Glaser, 2005). Considering a correlation matrix of the ^{13}C enrichment values helped to examine the sources of the different biomarkers (Table 4).

In the presented study, the Gram-positive bacterial markers (i15:0 was used as representative) correlated well with the Gram-negative bacterial markers (19:0cy was used as representative). The Actinomycetes marker 10Me17:0 behaved like both Gram-negative bacterial and Gram-positive bacterial biomarker, but the highest correlation was to the Gram-negative bacterial biomarker. All these markers behaved in the same way and seemed to be out of the bacterial pool. In contrast to the saturated Gram-negative bacterial biomarkers (17:0cy and 19:0cy), 16:1ω7 and 18:1ω7 showed a larger enrichment and different time course with ^{13}C

incorporation already immediately after labeling. They correlated the best to each other. Both Gram-negative bacterial biomarkers could have been mixed signals out of different pools. Or alternatively it could indicate different bacteria kinds. 16:1ω9 and 18:1ω5 correlated with all bacterial molecular markers. Both biomarkers are not widely used as specific biomarkers in existing literature and their source has not been clarified yet. The enrichment values laid in the range of the cyclopropyl biomarkers of Gram-negative bacteria, but the trend of 16:1ω9 was closer to the monounsaturated Gram-negative bacterial biomarker. The time pattern of 18:1ω5 indicated a small rising trend, like some biomarker of Gram-positive bacteria and had a high correlation with 16:1ω5. Both these markers displayed mixed signals from all bacterial types.

Analysis of PLFA 16:1ω5 enable an estimate of the AM fungi biomass in soil, but the peak always had a background signal between 30 and 60 %; mostly from bacteria (Olsson, 1999). PLFA 16:1ω5 is a good AMF marker when bacterial biomass is low; however, in this study the bacterial biomass was higher than the fungal biomass. The PLFA 16:1ω5 was correlated with the bacterial markers, suggesting the same pool origin. Additionally PLFA and NLFA 16:1ω5 displayed different patterns, which indicates an origin from different pools. Therefore, in the presented thesis it could be used as bacterial marker. At the excluded time points (T2C and T10A) the PLFA 16:1ω5 showed high ^{13}C enrichment and high standard deviations. This indicates an influence of AMF in the assumed biomarker for bacteria in the two soil samples, connected to a slightly higher concentration of the biomarker. PLFAs are membrane lipids whereas the NLFAs are used for energy storage (van Aarle and Olsson, 2003). AM fungi are known to store most of its energy as neutral lipids and usually have higher amounts of neutral lipids than phospholipids (Olsson and Johansen, 2000). Therefore, the NLFA 16:1ω5 is more sensitive than the PLFA marker as an indicator for AM fungi in soil and allows detecting low densities of AMF hyphae (Olsson, 1999). Without the excluded values, the NLFA 16:1ω5 behaved almost like the fungi marker 18:2ω6,9. 18:2ω6,9 and 18:1ω9 are not exclusive markers for fungi, but also found in plants (Frostegård et al., 2011). However, studies found a high correlation between PLFA 18:2ω6,9 and the fungal marker ergosterol, which makes 18:2ω6,9 a good fungi marker (Frostegard and Baath, 1996, Kaiser et al., 2010). Further extractions of PLFAs from several fungal fruit bodies of basidiomycetes from an ectomycorrhiza-dominated coniferous forest, exhibited that the PLFA pool is dominated by 18:2w6,9 (Baldrian et al., 2013). Relative contents of 18:2ω6,9 between 66.5 % and 96.6 % were found. At the presented thesis the general biomarker n16:0 was characterized by the fungi marker 18:2ω6,9. Because of the good correlation to the fungi biomarker, an origin of fungi is possible. The study of PLFA patterns in different fungi species has been shown, that n16:0 was highly abundant in several fungi species (Ruess et al., 2002, Baldrian et al., 2013). However, here the n16:0 occurred in a much higher concentration than the fungi

biomarker 18:2ω6,9. This suggests that n16:0 did not represent only fungal biomass but several organisms. The n16:0 marker is found in most cellmembranes of organisms (Denef et al., 2007).

18:1ω9 was neither correlated to the bacterial markers nor to the fungi marker. Also the concentration of these both markers, as seen in the results, was not correlated to each other. It could have been a signal from roots left in the soil samples. However, almost no signals of long chained fatty acids (>20 C) and long chain polyunsaturated acids were detected in the samples. These compounds are biomarkers from plant materials and nematodes and contribution of plant derived fatty acids and nematodes lipids to the results of this study in general is unlikely (Treonis et al., 2004). Most roots were removed prior extraction. This suggests that the biomarkers were predominantly from soil organisms. The unspecific biomarker n18:0 had the highest correlation with the molecular marker 16:1ω7, but also with n16:0. A very high correlation was not seen to any compound. n18:0 has not been known as a specific biomarker and has been found in several organisms. No clear clarification of this marker can be made. It seems to displayed many pools, and may be used as community marker.

4.4 Lipid biomarkers specific ^{13}C enrichment

Carbon deposits by root externals are an important source for microbes in the rhizosphere (Butler et al., 2003). Rhizodeposit compounds have a short turnover rate in soils because up to 86 % are respired by soil microbes within only a few days (Hütsch et al., 2002). Photosynthetically fixed carbon was incorporated rapidly into belowground soil microbial biomass. ^{14}C pulse-chase labeling indicated translocation of recent photoassimilated carbon into microbial between in less than 1 h after labeling (Rattray et al., 1995), suggesting a very rapidly moving of photosynthetically fixed carbon through the plant-microbial system (Balasooriya et al., 2012). The present study already showed immediately after the labeling ^{13}C enrichment signals in several markers (Figure 15). ^{13}C enrichment varied greatly among individual PLFAs and among the time course, suggesting different uptake rates of new rhizodeposit C by different microbial groups.

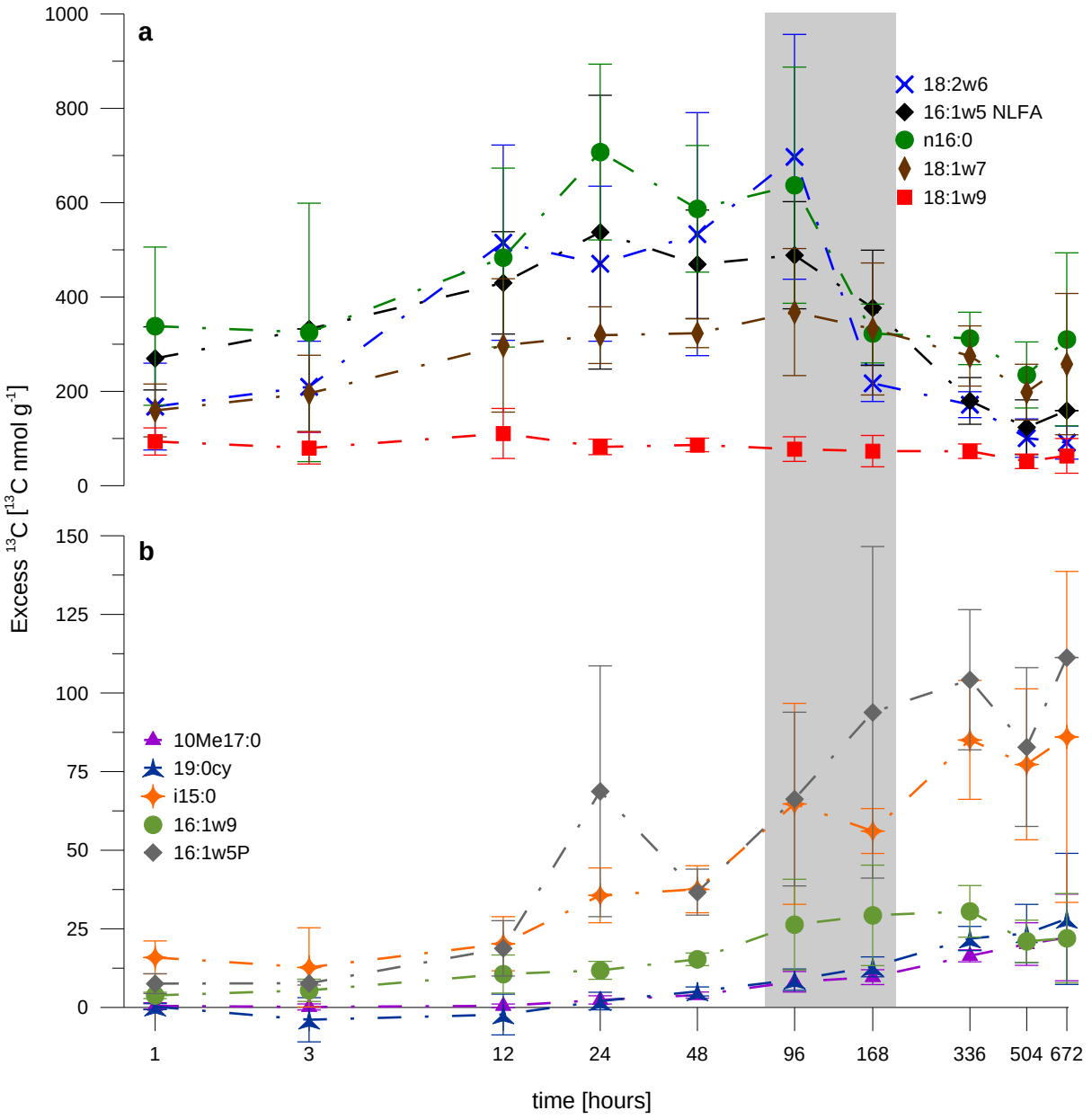

Figure 15: Excess ^{13}C of specific organism groups. The diagram displays the ^{13}C enrichment of all detected organism groups with one representative for each. (a) Shows the higher enriched markers with the fungi SF biomarker (18:2ω6,9) and general fungi biomarker (18:1ω9), AMF biomarker (NLFA 16:1ω5), community biomarker (n16:0) and MUFA Gram-negative bacterial biomarker (18:1ω7). (b) shows the Gram-positive bacterial biomarker (i15:0), cyclopropyl Gram-negative bacterial biomarker (19:0y) and biomarker of the Actinomycetes (10Me17:0). Additionally the PLFA 16:1ω5 and 16:1ω9 as bacterial biomarker are seen. The grey line indicates the coincidence of the gradual decrease of the fungi with the major labeling of the bacteria.

4.4.1 Fungal lipid biomarkers

In the presented study n16:0 followed the course of the fungi biomarker 18:2ω6,9 indicating a high influence of fungal lipids on this marker. n16:0 had the highest ^{13}C enrichment of all analyzed biomarkers. The high enrichment was observed in other pulse-chase studies and in labeled substrate addition experiments (Treonis et al., 2004, Williams et al., 2006, Jin and

Evans, 2010). Jin and Evans (2010) explained the high enrichment with its central role in the biosynthesis of vast majority of fatty acids and its occurrence among all eubacteria and higher organisms. After n16:0, saprophytic (18:2ω6,9) as well as AM fungi (NLFA 16:1ω5) molecular markers appeared to have the highest ^{13}C enrichment in soil. The high enrichment of these biomarkers was also described in other labeling studies, even when organic substrates like acetate were used (Boschker et al., 1998, Butler et al., 2003, Denef et al., 2007). AMF appeared to be the major contributor to the NLFA 16:1ω5 peak. Several studies highlighted the important role of AMF in soils carbon cycle and also showed a fast incorporation of newly rhizodeposited carbon (Johnson et al., 2002, Olsson and Johnson, 2005). AMF were defined as the major conduit in the transfer of carbon between plants and soil (Drigo et al., 2010). Fungi markers indicated the highest enrichment at the first sampling point compared to other PLFAs. This fast incorporation was also described by Treonis et al. (2004), who performed a $^{13}CO_2$-labeling experiment. The findings indicate a rapid uptake of assimilated plant–C in fungal communities and suggest fungi as the most actively microbe using plant deposited carbon (Butler et al., 2003). This finding fits together with the close growing of fungal hyphae to the root system (Butler et al., 2003). The results of the presented thesis and other studies of fungi ^{13}C enrichment indicate an important role of fungi in soils carbon cycle. Fungi have higher substrate assimilation efficiency than bacteria and are able to break down polymer substrates and complex polyaromatic compounds (Scheu et al., 2005). The high ^{13}C incorporation underlines the great substrate use efficiency of fungi (Zak et al., 1996). The ^{13}C enrichment of SF and AMF fungal markers displayed almost the same trend and showed enrichment around same values, suggesting an important role of both kinds of fungi, saprophytic and Arbuscular mycorrhizal, contrasting to the hypothesis that AMF play the major role in the carbon soil system.

In contrast to these both fungal markers, 18:1ω9 fungal lipid biomarker had small ^{13}C enrichment. The course of the incorporation differed from the other general fungal markers as has also been seen at the correlation matrix. The highest incorporation was reached at the first sampling point. The interpretation of this marker was difficult and a mixed signal seemed probable. Cellmembranes of fungi, Gram-positive bacteria and plants showed the occurrence of 18:1ω9 as well (Frostegard and Baath, 1996, Zelles, 1999).

4.4.2 Bacterial lipid biomarkers

The least enriched biomarkers were the Gram-positive bacterial, Actinomycetes and Gram-negative bacterial cyclopropyl molecular markers. Gram-positive bacterial compounds (anteiso- and iso-branched saturated lipids) had a small labeling at the beginning of the experiment and during the preceding experiment the enrichment got higher and was the highest at the end of the sampling period. The slow incorporation of labeled rhizodeposit ^{13}C

into bacteria was also found in several studies (Williams et al., 2006, Denef et al., 2009, Drigo et al., 2010). Also 17:0cy and 19:0cy showed a slow and very small enrichment like Gram-positive bacteria, but had no ^{13}C incorporation over the first time points at all. The first incorporation started 24 hours after labeling. Gram-negative bacteria convert monounsaturated components into cyclopropyl components under stress conditions and nutrient limitation (Kaur et al., 2005), the delayed enrichment could do to newly synthesized cyclopropyl components. However, the stable conditions in the pots over the time, should not lead to stress conditions. Also Actinomycetes were not enriched over the first four sampling points. They have been known for their slow growing (Drigo et al., 2010). It is possible that no label can be detected in these biomarkers because of inactivity and later growing of these bacteria. These variations in carbon uptake of bacterial molecular markers indicate different kinds of bacteria. Some bacteria depend greater on older SOM C, whereby the very low enrichment could be explained (Jin and Evans, 2010). Many bacteria in bulk soil are inactive until water or easily decomposable substrates become available (Scheu et al., 2005). Because of the temporal delayed incorporation of labeled ^{13}C it seemed that new rhizodeposit C is more slowly transferred to bacteria (Balasooriya et al., 2012) or that these microbial communities were active in metabolizing other sources of C than the newly produced rhizodeposits (Denef et al., 2007). These molecular markers seem to be indicators of saprophytic bacteria. The degradation of complex compounds by fungi releases simple molecules, which can be used by other soil organisms (Scheu et al., 2005) and AMF are known for their release of large amounts of glycoproteine and glomalin into the soil (Rillig et al., 2002). The finding that the gradual decrease of the ^{13}C enrichment in fungal markers coincided with the major labeling of the bacteria underlines the suggestion of saprophytic bacteria (Figure 15). Either they preferred the use of dead root and fungal necromass as C source or taking up carbon from degenerating C leaking of fungal hyphae (Denef et al., 2009). $^{13}CO_2$ pulse-chase labeling with AMF and no AMF showed that in the AMF system the majority of the ^{13}C is assimilated by the bacterial rhizosphere was derived from AMF turnover, because of the reverse trend of AMF and bacterial biomarkers (Drigo et al., 2010). In contrast, the non AMF system of bacterial lipids showed a rapid incorporation of rhizodeposited carbon. Earlier results displayed as well that the main plant deposit carbon was taken up by AMF, and only minor fractions reached the bacterial community (Olsson and Johnson, 2005).

In contrast to these results, the Gram-negative biomarkers 16:1ω7 and 18:1ω7 rapidly incorporated the root derivate carbon and had larger ^{13}C enrichments than other bacteria biomarkers. These Gram-negative bacteria seemed to be a main contributor of the plant derived carbon after fungi. These results indicate the presence of different bacteria kinds in soil. The Gram-positive bacteria seem to be saprophytic organisms which take up the fungi derived carbon and older carbon sources, some Gram-negative bacteria appear to play a minor

role in plant-soil carbon uptake and behave more inactive. Other Gram-negative bacteria play a more important role in recent photosynthetically fixed C uptake. It has been suggested that the breakdown of specific C compounds released by plants are associated to different microbial groups (Nielsen et al., 2011). Substrate label studies showed differences in utilization of C substrates among microbial communities (Paterson et al., 2007). They demonstrated that a significantly greater portion of ^{13}C-glycine was found in Gram-negative bacteria and a significantly lower proportion in Gram-positive bacteria, Actinomycetes and fungi. Bird et al. (2011) pointed out a preferentially use of older dead root debris as carbon source by Gram-positive bacteria. In general Gram-positive bacteria seem to use older material and Gram-negative bacteria prefer freshly rhizodeposit carbon. The differences in the uptake of recently photoassimilated carbon among the microbial communities could have important implications of C storage in terrestrial systems, because it was suggested that fungal mediated C storage is more persistent than bacterial C storage (Balasooriya et al., 2012).

4.5 Duration of ^{13}C enrichment of specific biomarkers

The ^{13}C enrichment of the identified fungal lipid biomarker 18:2ω6,9 was still largely present after four weeks but decreased relatively to the enrichment observed at the beginning. The same patterns were found in the AMF NLFA biomarker and 16:1ω7 and 18:1ω7 biomarkers of Gram-negative bacteria. The reason for the decreasing of the ^{13}C enrichment could be the dilution of the signal by the fresh unlabeled CO_2 gas after the labeling period. Mean residence time estimation of Balasooriya et al. (2012) and turnover rate estimation by Treonis et al. (2004) displayed different lifespans of different microbial groups or a possible translocation of photosynthetically fixed C among different communities. Several studies exposed a faster turnover of fungal biomarkers in contrast to bacterial biomarkers (Treonis, basay). In the presented thesis the AMF NLFA biomarker 16:1ω5 was still labeled after four weeks. Denef et al. (2007) found high ^{13}C enrichment in fungal biomarkers after 11 month, suggesting a continued fungal assimilation or recycling of ^{13}C labeled rhizodeposit carbon, due to still highly labeled root biomass found 11 month after the labeling period. In contrast, Drigo et al. (2010) showed that this marker was reaching the baseline again 14 days after labeling and analysis of AMF hyphae indicated a turnover rate of 5 to 6 days (Staddon et al., 2003). Because the study of Staddon et al., (2003) focused on C flux in extraradical hyphae close to the plant surface it can just make limited statements about residence time of AMF biomass in soil (Olsson and Johnson, 2005). A large fraction of rhizodeposit C is incorporated into fungal structural and storage compounds (i.e. NLFA compounds) (Olsson and Johnson, 2005). The long time period of ^{13}C enrichment in NLFA components suggest a longer residence time than 6 days (Olsson and Johnson, 2005). The Gram-positive markers got more enriched at the end of the sampling period and in total the bacterial biomass was

higher enriched than the fungal biomass after one week (Figure 16), suggesting a longer turnover time. The data demonstrate a relatively long period of freshly assimilated carbon in the soil system, indicating recycling of carbon in short time terms.

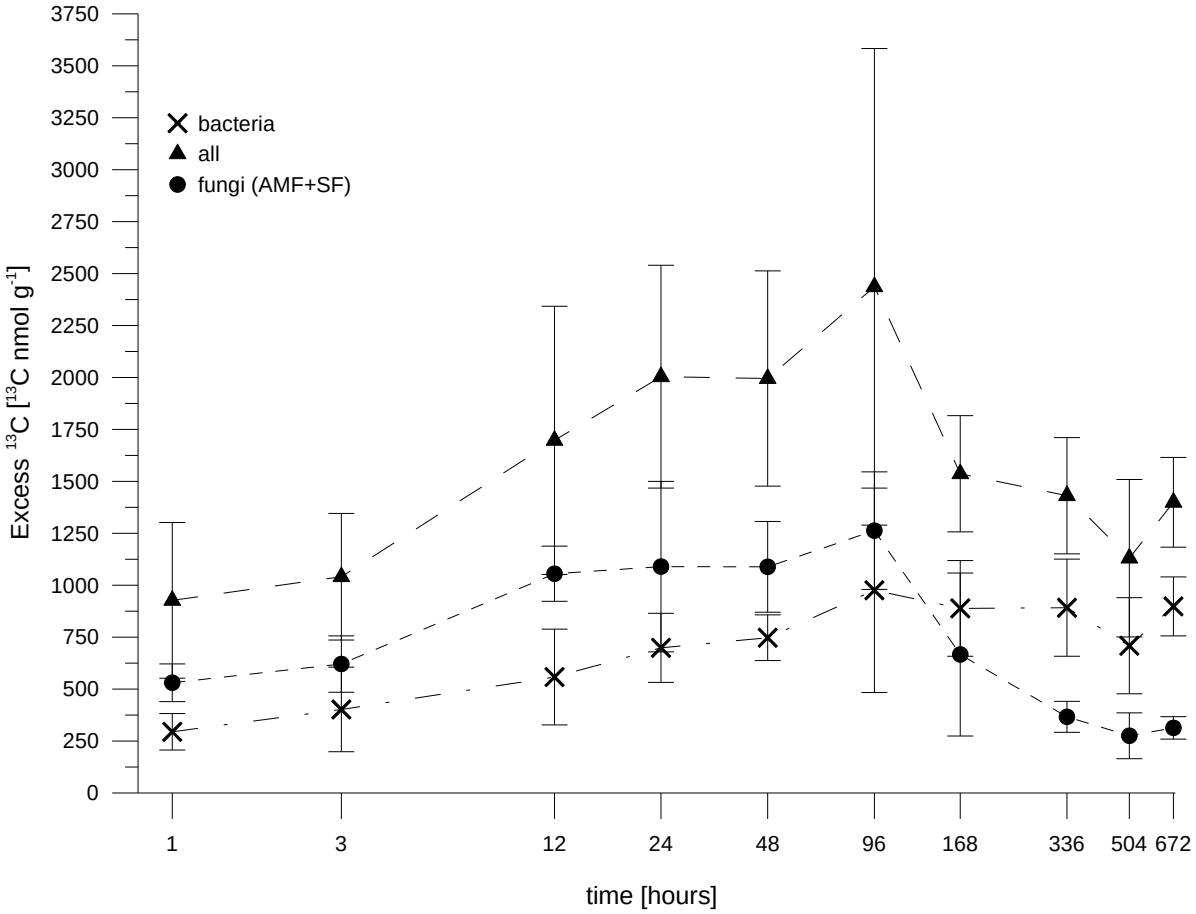

Figure 16: Bulk ^{13}C enrichment of the microbial communities. ^{13}C enrichment (^{13}C nmol g^{-1}) of the bacterial bulk (✕) determined as mean of the bacteria-specific PLFAs (i14:0, a15:0, i15:0, i16:0, a17:0, i17:0, 16:1ω5, 16:1ω7, 16:1ω9, 18:1ω5, 18:1ω7, 19:0cy, 17:0cy, 10Me17:0), fungal bulk (●) as mean of AMF NLFA and 18:2ω6,9 SF biomarkers and the bulk of the whole soil community (▲). The enrichment is plotted over the time based on a $\log_{10}$ scale.

4.6 Environmental inferences from carbon utilization

Microbial community patterns are changing over soil profiles (Fritze et al., 2000, Blume et al., 2002, Fierer et al., 2003). In general rhizosphere soil has higher biomass than the bulk soil (Soderberg et al., 2004). Fierer et al. (2003) used PLFA analysis to investigate changes in microbial communities over depth in soil profiles. They demonstrated that the composition of the soil microbial communities changed significantly with the depth. In general microbial communities shift from greater Gram-negative dominance at the soil surface to greater Gram-positive dominance at deeper soil depth. Gram-positive bacteria and Actinomycetes marker amounts increased with deeper soil depth, while Gram-negative bacteria, fungi and protozoa marker were highest in the subsurface soil and decreased at the shallowest depth. These results were also found in several other studies (Fritze et al., 2000, Blume et al., 2002, Taylor et al., 2002, Soderberg et al., 2004). The ratio of the sum of 17:0cy and 19:0cy to the sum of 16:1ω7 and 18:1ω7, which have been used as stress indicators (Bossio and Scow, 1998), was increasing over the depth in the study of Fierer et al. (2003). They hypothesize that soil resource availability was the main factor responsible for the observed changes in microbial community patterns over the depth. The carbon concentration was decreasing at higher depth; additionally a reduction of carbon quality with soil depth has been well known (Trumbore, 2000). The activity of microorganism in soil is usually limited by carbon, except in the rhizosphere where carbon is deposit constantly by plants (Scheu et al., 2005). The microbes in the rhizosphere seem to be able to utilize the new synthesized carbon in soil. As seen in the ^{13}C enrichment of the presented study, the mono unsaturated Gram-negative bacterial molecular markers differ in the carbon uptake pattern to the cyclopropyl molecular markers (17:0cy and 19:0cy). The mono unsaturated lipids were getting rapidly enriched, suggesting a fast incorporation of the photosynthetically fixed carbon. Therefore they rely on plant derived carbon, whereas the cyclopropyl components seem to use other sources of carbon in soil, because of the delayed enrichment observed. Further the bacteria presented by the cyclopropyl compounds seemed to be inactive over the first period of the experiment. These microbes are more dependent on older SOM carbon. With the data of the presented thesis, the use of the ratio 17:0cy+19:0cy/16:1ω7+18ω7 as stress indicator could be explained by the different metabolism of these microbes. Also the dominant occurrence of Gram-positive bacteria in deeper soil layers seemed due to the better adaption of low carbon availability.

5 Conclusion

This study shows short time series sampling of a $^{13}CO_2$ pulse-chase labeling over a sampling period of four weeks. Better insight into the interaction between plants and the soil system on a short scale of the carbon were obtained. The data underline the finding of the fast process of freshly assimilated carbon in the soil system and the predominantly role of fungi in the carbon cycle in terrestrial systems. The use of PLFA to identify microbial groups and their metabolic activity needs attention. Sources of several biomarkers are not clarified and most of the biomarkers occur in different organism groups. When working with PLFA it is important to clarify the source organism. Some biomarker assumed to originate from the same pool showed deviating behavior in carbon uptake patterns, which makes an interpretation difficult. The identification of specific species involved in the carbon cycle, helps to get more detailed insights into belowground carbon processes. Because the soil is a very complex and fast changing system the ^{13}C incorporation between replicates varied a lot. More replicates should be used for ^{13}C labeling studies to get lower standard deviations to provide more reliable data.

Rhizodeposit is an important carbon source for the soil micro fauna. The results demonstrate that $^{13}CO_2$ pulse-chase labeling coupled to lipid analysis is a useful tool to gain insights into the carbon cycle from atmosphere into belowground soil communities. It can reveal structural information of the microbial communities actively involved in cycling of rhizodeposited C. The results confirm the rapid carbon flow of recently photosynthetically fixed carbon by plants into soil microbial communities. Within 1h after the pulse labeling ^{13}C enrichment was found in the soil biomass. Fatty acids indicative for saprophytic and AM fungi and Gram-negative bacteria showed high ^{13}C enrichment indicating a strong relationship to rhizodeposited carbon compared to Gram-positive bacteria and Actinomycetes. Fungi have the highest ^{13}C enrichment, hence are the main receiver of rhizodeposit carbon. The predominantly role of AMF could not be fully clarified by the data. Also saprophytic fungi seem to play an important role in plant-soil carbon transfer. The ^{13}C enrichment of the Gram-positive bacterial and Actinomycetes biomarkers occurred with some delay, indicating a slower transport of the rhizodeposit carbon into these communities by a fungal mediated carbon transfer via degenerated fungal hyphae or preferred use of older SOM. These results displayed two kinds of bacteria in the soil system. The saprophytic bacteria and rhizodeposit relied bacteria. Further research of preferential substrate utilization by different organisms would help to get more detailed knowledge about carbon processes in soil and the actively involved organism species.

Comparing data of carbon utilization patterns in other $^{13}CO_2$ labeling studies and soil ecosystem studies helps to connect the carbon metabolism to environmental behavior of specific microbial communities. Gram-negative bacteria could be divided and associated with different behavior in the environment. The cyclopropyl components had slower and smaller

^{13}C enrichment than their precursors 16:7ω7 and 18:1ω7, which directly take up rhizodeposit carbon. Fungi play an important role in the carbon cycle in soil, especially of rhizodeposited carbon, but also bacteria seem to be an important factor of the rhizodeposit carbon cycle. The long duration of ^{13}C enrichment of the different specific biomarkers indicates different persistence of microbial groups. Furthermore it shows a recycling of the carbon recently fixed by photosynthesis. The estimation of turnover rates of the different molecular markers would help to make more detailed statements about lifespans of different microbes.

6 References

Alexander, M. (1977) Introduction to soil microbiology. John Wiley & Sons.

Balasooriya, W. K., Denef, K., Huygens, D., and Boeckx, P. (2012) Translocation and turnover of rhizodeposit carbon within soil microbial communities of an extensive grassland ecosystem. Plant and Soil:1-13.

Baldrian, P., Větrovský, T., Cajthaml, T., Dobiášová, P., Petránková, M., Šnajdr, J., and Eichlerová, I. (2013) Estimation of fungal biomass in forest litter and soil. Fungal Ecology **6**:1-11.

Baugh, P. J. (1993) Gas Chromatography: a practical approach. IRL Press at Oxford University Press Oxford.

Bird, J. A., Herman, D. J., and Firestone, M. K. (2011) Rhizosphere priming of soil organic matter by bacterial groups in a grassland soil. Soil Biology & Biochemistry **43**:718-725.

Bligh, E. G. and Dyer, W. J. (1959) A rapid method of total lipid extraction and purification. Canadian Journal of Biochemistry and Physiology **37**:911-917.

Blume, E., Bischoff, M., Reichert, J. M., Moorman, T., Konopka, A., and Turco, R. F. (2002) Surface and subsurface microbial biomass, community structure and metabolic activity as a function of soil depth and season. Applied Soil Ecology **20**:171-181.

Boschker, H. T. S. and Middelburg, J. J. (2002) Stable isotopes and biomarkers in microbial ecology. FEMS Microbiology Ecology **40**:85-95.

Boschker, H. T. S., Nold, S. C., Wellsbury, P., Bos, D., de Graaf, W., Pel, R., Parkes, R. J., and Cappenberg, T. E. (1998) Direct linking of microbial populations to specific biogeochemical processes by C-13-labelling of biomarkers. Nature **392**:801-805.

Bossio, D. A. and Scow, K. M. (1998) Impacts of carbon and flooding on soil microbial communities: Phospholipid fatty acid profiles and substrate utilization patterns. Microbial Ecology **35**:265-278.

Butler, J. L., Williams, M. A., Bottomley, P. J., and Myrold, D. D. (2003) Microbial community dynamics associated with rhizosphere carbon flow. Applied and Environmental Microbiology **69**:6793-6800.

Cardon, Z. G., Hungate, B. A., Cambardella, C. A., Chapin Iii, F. S., Field, C. B., Holland, E. A., and Mooney, H. A. (2001) Contrasting effects of elevated CO2 on old and new soil carbon pools. Soil Biology and Biochemistry **33**:365-373.

Denef, K., Bubenheim, H., Lenhart, K., Vermeulen, J., Van Cleemput, O., Boeckx, P., and Muller, C. (2007) Community shifts and carbon translocation within metabolically-active rhizosphere microorganisms in grasslands under elevated CO2. Biogeosciences **4**:769-779.

Denef, K., Roobroeck, D., Wadu, M. C. W. M., Lootens, P., and Boeckx, P. (2009) Microbial community composition and rhizodeposit-carbon assimilation in differently managed temperate grassland soils. Soil Biology & Biochemistry **41**:144-153.

Drigo, B., Anderson, I. C., Kannangara, G. S. K., Cairney, J. W. G., and Johnson, D. (2012) Rapid incorporation of carbon from ectomycorrhizal mycelial necromass into soil fungal communities. Soil Biology & Biochemistry **49**:4-10.

Drigo, B., Pijl, A. S., Duyts, H., Kielak, A., Gamper, H. A., Houtekamer, M. J., Boschker, H. T. S., Bodelier, P. L. E., Whiteley, A. S., van Veen, J. A., and Kowalchuk, G. A. (2010) Shifting carbon flow from roots into associated microbial communities in response to elevated atmospheric CO2. Proceedings of the National Academy of Sciences of the United States of America **107**:10938-10942.

Ehleringer, J. R., Buchmann, N., and Flanagan, L. B. (2000) Carbon isotope ratios in belowground carbon cycle processes. Ecological Applications **10**:412-422.

Farquhar, G. D., Ehleringer, J. R., and Hubick, K. T. (1989) Carbon isotope discrimination and photosynthesis. Annual Review of Plant Physiology and Plant Molecular Biology **40**:503-537.

Fierer, N., Schimel, J. P., and Holden, P. A. (2003) Variations in microbial community composition through two soil depth profiles. Soil Biology and Biochemistry **35**:167-176.

Finlay, R. D. (2008) Ecological aspects of mycorrhizal symbiosis: with special emphasis on the functional diversity of interactions involving the extraradical mycelium. Journal of Experimental Botany **59**:1115-1126.

Frey-Klett, P., Garbaye, J., and Tarkka, M. (2007) The mycorrhiza helper bacteria revisited. New Phytologist **176**:22-36.

Fritze, H., Pietikainen, J., and Pennanen, T. (2000) Distribution of microbial biomass and phospholipid fatty acids in Podzol profiles under coniferous forest. European Journal of Soil Science **51**:565-573.

Frostegard, A. and Baath, E. (1996) The use of phospholipid fatty acid analysis to estimate bacterial and fungal biomass in soil. Biology and Fertility of Soils **22**:59-65.

Frostegård, Å., Tunlid, A., and Bååth, E. (2011) Use and misuse of PLFA measurements in soils. Soil Biology and Biochemistry **43**:1621-1625.

Glaser, B. (2005) Compound-specific stable-isotope (delta C-13) analysis in soil science. Journal of Plant Nutrition and Soil Science **168**:633-648.

Hütsch, B. W., Augustin, J., and Merbach, W. (2002) Plant rhizodeposition — an important source for carbon turnover in soils. Journal of Plant Nutrition and Soil Science **165**:397-407.

Jin, V. L. and Evans, R. D. (2010) Microbial 13C utilization patterns via stable isotope probing of phospholipid biomarkers in Mojave Desert soils exposed to ambient and elevated atmospheric CO2. Global Change Biology **16**:2334-2344.

Johnson, D., Leake, J. R., Ostle, N., Ineson, P., and Read, D. J. (2002) In situ (CO2)-C-13 pulse-labelling of upland grassland demonstrates a rapid pathway of carbon flux from arbuscular mycorrhizal mycelia to the soil. New Phytologist **153**:327-334.

Johnston, C. A., Groffman, P., Breshears, D. D., Cardon, Z. G., Currie, W., Emanuel, W., Gaudinski, J., Jackson, R. B., Lajtha, K., Nadelhoffer, K., Nelson, D., Post, W. M., Retallack, G., and Wielopolski, L. (2004) Carbon cycling in soil. Frontiers in Ecology and the Environment **2**:522-528.

Jones, D. L., Hodge, A., and Kuzyakov, Y. (2004) Plant and mycorrhizal regulation of rhizodeposition. New Phytologist **163**:459-480.

Jones, D. L., Nguyen, C., and Finlay, R. D. (2009) Carbon flow in the rhizosphere: carbon trading at the soil-root interface. Plant and Soil **321**:5-33.

Kaiser, C., Frank, A., Wild, B., Koranda, M., and Richter, A. (2010) Negligible contribution from roots to soil-borne phospholipid fatty acid fungal biomarkers 18:2ω6,9 and 18:1ω9. Soil Biology and Biochemistry **42**:1650-1652.

Kandeler, E., Stemmer, M., and Gerzabek, M. (2005) Role of microorganisms in carbon cycling in soils. Pages 139-157 *in* A. Varma and F. Buscot, editors. Microorganisms in Soils: Roles in Genesis and Functions. Springer Berlin Heidelberg.

Kaur, A., Chaudhary, A., Kaur, A., Choudhary, R., and Kaushik, R. (2005) Phospholipid fatty acid - A bioindicator of environment monitoring and assessment in soil ecosystem. Current Science **89**:1103-1112.

Kreuzer-Martin, H. W. (2007) Stable isotope probing: Linking functional activity to specific members of microbial communities. Soil Science Society of America Journal **71**:611-619.

Lal, R. (2008) Carbon sequestration. Philosophical Transactions of the Royal Society B-Biological Sciences **363**:815-830.

Lu, Y., Abraham, W. R., and Conrad, R. (2007) Spatial variation of active microbiota in the rice rhizosphere revealed by in situ stable isotope probing of phospholipid fatty acids. Environmental Microbiology **9**:474-481.

Lynch, J. M. and Whipps, J. M. (1990) Substrate flow in the rhizosphere. Plant and Soil **129**:1-10.

Mooney, H. A., Drake, B. G., Luxmoore, R. J., Oechel, W. C., and Pitelka, L. F. (1991) Predicting ecosystem responses to elevated CO2 concentrations. Bioscience **41**:96-104.

Nielsen, U. N., Ayres, E., Wall, D. H., and Bardgett, R. D. (2011) Soil biodiversity and carbon cycling: a review and synthesis of studies examining diversity-function relationships. European Journal of Soil Science **62**:105-116.

Olsson, P. A. (1999) Signature fatty acids provide tools for determination of the distribution and interactions of mycorrhizal fungi in soil. FEMS Microbiology Ecology **29**:303-310.

Olsson, P. A., Bååth, E., Jakobsen, I., and Söderström, B. (1995) The use of phospholipid and neutral lipid fatty acids to estimate biomass of arbuscular mycorrhizal fungi in soil. Mycological Research **99**:623-629.

Olsson, P. A. and Johansen, A. (2000) Lipid and fatty acid composition of hyphae and spores of arbuscular mycorrhizal fungi at different growth stages. Mycological Research **104**:429-434.

Olsson, P. A. and Johnson, N. C. (2005) Tracking carbon from the atmosphere to the rhizosphere. Ecology Letters **8**:1264-1270.

Paterson, E., Gebbing, T., Abel, C., Sim, A., and Telfer, G. (2007) Rhizodeposition shapes rhizosphere microbial community structure in organic soil. New Phytologist **173**:600-610.

Rattray, E. S., Paterson, E., and Killham, K. (1995) Characterisation of the dynamics of C-partitioning within Lolium perenne and to the rhizosphere microbial biomass using 14C pulse chase. Biology and Fertility of Soils **19**:280-286.

Rillig, M. C., Wright, S. F., and Eviner, V. T. (2002) The role of arbuscular mycorrhizal fungi and glomalin in soil aggregation: comparing effects of five plant species. Plant and Soil **238**:325-333.

Ruess, L. and Chamberlain, P. M. (2010) The fat that matters: Soil food web analysis using fatty acids and their carbon stable isotope signature. Soil Biology & Biochemistry **42**:1898-1910.

Ruess, L., Häggblom, M. M., García Zapata, E. J., and Dighton, J. (2002) Fatty acids of fungi and nematodes—possible biomarkers in the soil food chain? Soil Biology and Biochemistry **34**:745-756.

Scheu, S., Ruess, L., and Bonkowski, M. (2005) Interactions between microorganisms and soil micro-and mesofauna. Pages 253-275 Microorganisms in Soils: Roles in Genesis and Functions. Springer.

Schimel, D. S. (1995) Terrestrial ecosystems and the carbon cycle. Global Change Biology **1**:77-91.

Soderberg, K. H., Probanza, A., Jumpponen, A., and Baath, E. (2004) The microbial community in the rhizosphere determined by community-level physiological profiles (CLPP) and direct soil- and cfu-PLFA techniques. Applied Soil Ecology **25**:135-145.

Staddon, P. L., Ramsey, C. B., Ostle, N., Ineson, P., and Fitter, A. H. (2003) Rapid turnover of hyphae of mycorrhizal fungi determined by AMS microanalysis of 14C. Science **300**:1138-1140.

Taylor, J. P., Wilson, B., Mills, M. S., and Burns, R. G. (2002) Comparison of microbial numbers and enzymatic activities in surface soils and subsoils using various techniques. Soil Biology & Biochemistry **34**:387-401.

Torsvik, V., Goksoyr, J., and Daae, F. L. (1990) High diversity in DNA of soil bacteria. Applied and Environmental Microbiology **56**:782-787.

Treonis, A. M., Ostle, N. J., Stott, A. W., Primrose, R., Grayston, S. J., and Ineson, P. (2004) Identification of groups of metabolically-active rhizosphere microorganisms by stable isotope probing of PLFAs. Soil Biology & Biochemistry **36**:533-537.

Trumbore, S. (2000) Age of soil organic matter and soil respiration: Radiocarbon constraints on belowground C dynamics. Ecological Applications **10**:399-411.

van Aarle, I. M. and Olsson, P. A. (2003) Fungal lipid accumulation and development of mycelial structures by two Arbuscular mycorrhizal fungi. Applied and Environmental Microbiology **69**:6762-6767.

van Veen, J., Merckx, R., and van de Geijn, S. (1989) Plant-and soil related controls of the flow of carbon from roots through the soil microbial biomass. Plant and Soil **115**:179-188.

Williams, M. A., Myrold, D. D., and Bottomley, P. J. (2006) Carbon flow from 13C-labeled straw and root residues into the phospholipid fatty acids of a soil microbial community under field conditions. Soil Biology and Biochemistry **38**:759-768.

Zak, D. R., Ringelberg, D. B., Pregitzer, K. S., Randlett, D. L., White, D. C., and Curtis, P. S. (1996) Soil microbial communities beneath Populus grandidentata grown under elevated atmospheric CO_2. Ecological Applications:257-262.

Zelles, L. (1997) Phospholipid fatty acid profiles in selected members of soil microbial communities. Chemosphere **35**:275-294.

Zelles, L. (1999) Fatty acid patterns of phospholipids and lipopolysaccharides in the characterisation of microbial communities in soil: a review. Biology and Fertility of Soils **29**:111-129.

Zelles, L., Bai, Q. Y., Beck, T., and Beese, F. (1992) Signature fatty-acids in phospholipids and lipopolysaccharides as indicators of microbial biomass and community structure in Agricultural Soils. Soil Biology & Biochemistry **24**:317-323.

Zou, J., Liu, X., He, C., Zhang, X., Zhong, C., Wang, C., and Wei, J. (2013) Effect of Scripus triqueter of its rhizosphere and root exudates on microbial community structure of simulated diesel-spiked wetland. International Biodeterioration & Biodegradation **82**:110-116.

7 Appendix

Table A 1: Weigh determination of the different parameters for each sample.

	Wet weight g	Dry weight g	Water content %	Soil: Wet weight g	Soil: Dry weight g	K_2HPO_4 Buffer mL
T 1 A	4,99	3,99	20,0	62,53	50,00	37,5
T 1 B	5,12	3,95	22,9	64,81	50,00	35,2
T 1 C	5,04	3,88	23,0	65,10	50,15	35,1
T 2 A	5,01	4,18	16,6	59,93	50,00	40,1
T 2 B	4,97	3,87	22,1	64,21	50,00	35,8
T 2 C	4,99	4,11	17,6	60,71	50,00	39,3
T 3 A	5,00	3,89	22,2	64,27	50,00	35,7
T 3 B	5,00	3,93	21,4	63,61	50,00	36,4
T 3 C	5,06	4,17	17,6	60,67	50,00	39,3
T 4 A	5,15	4,21	18,3	61,16	50,00	38,8
T 4 B	5,07	4,14	18,3	61,23	50,00	38,8
T 4 C	4,96	3,97	20,0	62,47	50,00	37,5
T 5 A	5,10	4,33	15,1	61,07	52,18	40,8
T 5 B	5,09	4,15	18,5	61,57	50,24	38,6
T 5 C	5,09	3,95	22,4	64,63	50,20	35,5
T 6 A	5,01	4,16	17,0	63,48	53,26	39,2
T 6 B	5,11	4,04	20,9	63,24	50,00	36,8
T 6 C	5,06	4,05	20,0	62,47	50,00	37,5
T 7 A	5,03	4,16	17,3	67,50	57,04	38,3
T 7 B	5,08	3,79	25,4	67,22	50,20	32,9
T 7 C	5,08	4,09	19,5	62,94	50,84	37,7
T 8 A	5,06	4,07	19,6	62,10	49,94	37,9
T 8 B	5,13	4,09	20,3	62,34	49,63	37,4
T 8 C	5,03	3,99	20,7	63,46	50,43	36,9
T 9 A	4,99	3,97	20,4	63,11	50,26	37,1
T 9 B	5,04	4,09	18,8	63,11	51,50	38,1
T 9 C	5,13	4,12	19,7	63,56	51,30	37,5
T 10 A	5,09	4,26	16,3	59,84	50,10	40,2
T 10 B	5,26	4,33	17,7	60,95	50,21	39,2
CON A	5,31	4,51	15,1	58,85	49,98	41,1
CON B	5,01	4,30	14,2	58,32	50,06	41,7
CON C	5,09	4,24	16,7	60,80	50,78	39,8

Table A 2a: Concentration of all detected PLFAs in mol%.

	T1A	±σ	T1B	±σ	T1C	±σ	T2A	±σ	T2B	±σ	T2C	±σ	T3A	±σ	T3B	±σ	T3C	±σ	T4A	±σ	T4B	±σ	T4C	±σ
i14:0	2.04	0.01	1.89	0.02	1.97	0.01	1.91	0.00	0.10	0.00	2.17	0.02	1.56	0.01	2.03	0.01	1.21	0.01	2.13	0.00	1.95	0.02	2.22	0.01
n14:0	0.78	0.01	0.66	0.00	0.65	0.00	0.57	0.01	0.00	0.00	0.82	0.00	0.49	0.00	0.74	0.01	0.39	0.00	0.84	0.01	0.75	0.00	0.88	0.00
i15:0	6.73	0.05	6.45	0.16	6.63	0.02	6.59	0.05	2.51	0.02	7.45	0.06	5.92	0.02	6.75	0.01	4.24	0.05	6.99	0.04	6.80	0.04	6.98	0.22
a15:0	5.35	0.03	4.68	0.03	4.90	0.01	4.81	0.00	1.84	0.01	5.43	0.03	4.39	0.03	4.99	0.01	3.13	0.03	5.25	0.02	5.00	0.03	5.16	0.06
n15:0	0.24	0.00	0.15	0.00	0.12	0.01	0.07	0.00	0.00	0.00	0.21	0.00	0.04	0.00	0.22	0.01	0.06	0.00	0.28	0.02	0.25	0.00	0.32	0.00
10Me16	0.19	0.00	0.12	0.00	0.20	0.00	0.00	0.00	0.00	0.00	0.00	0.00	0.00	0.00	0.04	0.04	0.00	0.00	0.16	0.02	0.05	0.00	0.14	0.04
i16:0	2.02	0.01	1.66	0.01	1.74	0.01	1.66	0.00	0.93	0.01	2.03	0.01	1.56	0.01	1.91	0.01	1.10	0.01	2.03	0.00	1.89	0.00	2.01	0.00
n16:0	10.85	0.05	10.22	0.09	10.63	0.02	10.69	0.00	6.92	0.07	11.95	0.02	9.63	0.04	10.52	0.01	6.20	0.07	10.32	0.07	9.66	0.02	10.51	0.02
17:0br	0.63	0.00	0.54	0.02	0.56	0.00	0.46	0.00	0.25	0.00	0.67	0.00	0.39	0.01	0.62	0.04	0.28	0.01	0.68	0.01	0.63	0.00	0.66	0.01
10Me17	5.91	0.02	5.51	0.05	5.92	0.02	5.58	0.01	4.07	0.03	6.29	0.01	5.42	0.31	5.76	0.00	3.43	0.03	5.66	0.03	5.35	0.01	5.94	0.00
i17:0	1.89	0.05	1.64	0.01	1.68	0.01	1.68	0.05	1.23	0.01	1.95	0.01	1.55	0.00	1.82	0.02	1.02	0.01	1.82	0.01	1.76	0.00	2.12	0.01
a17:0	1.71	0.02	1.50	0.02	1.56	0.00	1.46	0.00	1.06	0.00	1.70	0.01	1.30	0.00	1.61	0.01	0.89	0.00	1.65	0.00	1.53	0.01	1.82	0.01
17:0cy	2.18	0.01	2.05	0.02	2.09	0.00	2.04	0.01	1.40	0.01	2.40	0.01	1.78	0.01	2.16	0.01	1.25	0.01	2.18	0.00	2.11	0.01	2.32	0.01
10Me18	0.74	0.00	0.59	0.01	0.59	0.00	0.52	0.01	0.45	0.00	0.67	0.00	0.47	0.01	0.74	0.00	0.41	0.00	0.82	0.01	0.76	0.01	0.79	0.01
n18:0	2.16	0.00	1.95	0.01	1.93	0.01	1.91	0.00	1.66	0.01	2.18	0.01	1.72	0.00	2.01	0.00	1.08	0.01	1.98	0.01	1.82	0.01	2.09	0.02
19:0br	1.20	0.01	1.02	0.01	1.01	0.00	0.99	0.01	0.90	0.00	1.15	0.02	0.92	0.01	1.15	0.01	0.66	0.00	1.20	0.02	1.16	0.00	1.22	0.01
19:0cy	6.00	0.03	5.23	0.04	5.29	0.03	5.21	0.01	4.39	0.01	5.89	0.01	4.55	0.01	5.23	0.01	3.02	0.05	5.03	0.00	4.71	0.02	5.38	0.05
n21:0	0.31	0.01	0.27	0.00	0.22	0.02	0.20	0.00	0.25	0.01	0.28	0.00	0.17	0.01	0.34	0.01	0.15	0.01	0.36	0.01	0.34	0.00	0.44	0.00
C15:1	0.68	0.00	0.67	0.01	0.71	0.01	0.28	0.20	0.55	0.00	0.02	0.01	0.27	0.01	0.43	0.01	0.77	0.01	0.50	0.00	0.44	0.00	0.67	0.14
16:1ω9c	1.37	0.00	1.46	0.01	1.46	0.01	1.43	0.08	2.33	0.03	0.76	0.05	1.53	0.02	1.47	0.05	2.45	0.00	1.71	0.03	1.74	0.03	1.74	0.02
16:1ω7c	7.10	0.01	7.84	0.03	8.04	0.16	7.27	0.01	11.49	0.06	4.44	0.01	8.56	0.01	7.46	0.03	11.64	0.18	7.99	0.04	8.80	0.01	8.09	0.04
16:1ω5c	4.43	0.01	4.70	0.01	4.77	0.10	4.21	0.02	7.18	0.02	2.73	0.00	5.16	0.01	4.53	0.02	6.99	0.10	4.89	0.03	5.22	0.01	4.98	0.03
C17:1	3.65	0.01	3.58	0.02	3.80	0.18	3.19	0.02	4.93	0.21	2.25	0.00	3.83	0.01	3.46	0.01	5.39	0.06	3.47	0.13	3.93	0.01	3.68	0.03
17:1ω7c	0.41	0.04	0.32	0.01	0.29	0.00	0.13	0.01	0.59	0.03	0.16	0.02	0.36	0.06	0.44	0.03	0.80	0.03	0.55	0.02	0.58	0.01	0.56	0.00
18:1ω9c	7.05	0.03	7.27	0.06	7.42	0.01	6.71	0.04	10.39	0.03	5.81	0.04	8.07	0.01	7.03	0.00	10.68	0.01	7.42	0.01	7.69	0.03	7.64	0.05
18:1ω7c	11.55	0.08	12.37	0.24	12.63	0.12	11.55	0.09	17.86	0.05	9.74	0.09	13.42	0.02	11.65	0.01	17.60	0.03	12.43	0.02	12.65	0.05	12.81	0.08
18:1ω5c	0.91	0.02	0.95	0.03	0.96	0.03	0.74	0.01	1.48	0.01	0.73	0.00	0.92	0.00	1.00	0.00	1.52	0.02	1.06	0.00	1.02	0.00	1.17	0.01
C19:1	0.69	0.00	0.72	0.00	0.68	0.00	0.57	0.01	1.08	0.01	0.58	0.00	0.72	0.03	0.71	0.00	1.18	0.01	0.70	0.00	0.89	0.01	0.84	0.00
20:1ω9c	0.38	0.01	0.33	0.15	0.41	0.01	0.25	0.01	0.70	0.02	0.28	0.13	0.37	0.01	0.43	0.00	0.74	0.02	0.53	0.01	0.53	0.03	0.58	0.00
18:2ω6c	1.41	0.00	1.66	0.01	1.28	0.06	1.37	0.00	1.04	0.00	1.97	0.01	1.84	0.04	1.46	0.00	2.06	0.20	1.55	0.00	1.43	0.03	1.37	0.02
18:3ω3	0.15	0.01	0.15	0.00	0.00	0.00	0.00	0.00	0.44	0.00	0.38	0.07	0.25	0.05	0.27	0.00	0.38	0.00	0.22	0.00	0.42	0.00	0.18	0.00
C20:4ω6	0.40	0.00	0.51	0.00	0.43	0.01	0.40	0.00	0.35	0.00	0.80	0.00	0.53	0.00	0.44	0.00	0.50	0.03	0.49	0.00	0.33	0.01	0.51	0.01

Table A 2b: Concentration of all detected PLFAs in mol%.

	T5A	±σ	T5B	±σ	T5C	±σ	T6A	±σ	T6B	±σ	T6C	±σ	T7A	±σ	T7B	±σ	T7C	±σ	T8A	±σ	T8B	±σ	T8C	±σ
i14:0	1.84	0.03	2.13	0.01	1.84	0.02	1.90	0.04	2.11	0.03	1.82	0.00	1.29	0.01	1.38	0.01	1.70	0.00	2.00	0.01	1.95	0.01	1.72	0.00
n14:0	0.68	0.00	0.81	0.00	0.66	0.01	0.78	0.02	0.86	0.01	0.75	0.00	0.54	0.00	0.62	0.00	0.69	0.00	0.80	0.00	0.79	0.01	0.68	0.00
i15:0	6.32	0.10	6.83	0.07	5.95	0.02	6.27	0.19	6.78	0.09	5.89	0.07	4.25	0.02	5.71	0.03	5.31	0.01	6.62	0.03	6.35	0.02	5.88	0.15
a15:0	4.77	0.07	5.03	0.04	4.33	0.02	4.69	0.08	4.94	0.06	4.28	0.05	3.13	0.02	4.28	0.02	3.93	0.00	4.89	0.02	4.72	0.02	4.30	0.06
n15:0	0.24	0.00	0.29	0.00	0.23	0.01	0.31	0.01	0.36	0.01	0.28	0.00	0.23	0.00	0.29	0.01	0.25	0.00	0.33	0.00	0.32	0.00	0.28	0.00
10Me16	0.14	0.01	0.25	0.00	0.15	0.00	0.26	0.01	0.21	0.00	0.19	0.00	0.15	0.00	0.10	0.03	0.20	0.00	0.25	0.00	0.26	0.03	0.23	0.00
i16:0	1.72	0.03	1.98	0.00	1.69	0.01	1.84	0.03	1.92	0.01	1.67	0.00	1.19	0.01	1.84	0.01	1.53	0.00	1.92	0.00	1.86	0.01	1.65	0.00
n16:0	9.37	0.17	10.20	0.04	8.94	0.05	9.80	0.04	9.88	0.06	9.01	0.01	6.61	0.03	10.20	0.04	8.49	0.01	9.96	0.00	9.79	0.03	8.79	0.03
17:0br	0.60	0.01	0.66	0.01	0.58	0.01	0.68	0.01	0.71	0.00	0.62	0.00	0.47	0.00	0.70	0.00	0.58	0.00	0.71	0.00	0.66	0.00	0.64	0.01
10Me17	5.33	0.06	5.47	0.01	4.89	0.03	5.20	0.03	5.32	0.01	4.80	0.00	3.67	0.01	5.52	0.02	4.64	0.00	5.54	0.01	5.22	0.03	5.04	0.03
i17:0	1.64	0.03	1.82	0.00	1.66	0.12	1.73	0.01	1.79	0.03	1.61	0.01	1.20	0.01	1.86	0.00	1.45	0.01	1.87	0.02	1.80	0.02	1.66	0.03
a17:0	1.45	0.03	1.61	0.00	1.46	0.04	1.55	0.01	1.59	0.01	1.43	0.00	1.06	0.00	1.68	0.01	1.34	0.00	1.62	0.00	1.57	0.00	1.44	0.01
17:0cy	2.10	0.04	2.19	0.01	1.97	0.02	2.07	0.02	2.15	0.01	1.90	0.00	1.42	0.02	2.16	0.02	1.78	0.01	2.14	0.01	2.11	0.00	1.99	0.01
10Me18	0.61	0.01	0.74	0.00	0.66	0.00	0.76	0.01	0.82	0.00	0.70	0.00	0.43	0.01	0.75	0.01	0.57	0.01	0.76	0.00	0.73	0.00	0.65	0.00
n18:0	1.83	0.03	2.00	0.01	1.75	0.00	1.89	0.01	1.94	0.00	1.78	0.00	1.33	0.00	2.14	0.00	1.69	0.00	1.97	0.01	1.95	0.00	1.75	0.00
19:0br	1.04	0.03	1.22	0.01	1.07	0.00	1.18	0.01	1.23	0.00	1.04	0.01	0.73	0.00	1.26	0.01	0.94	0.00	1.18	0.01	1.15	0.00	1.04	0.01
19:0cy	5.28	0.12	5.39	0.02	4.79	0.01	5.02	0.00	5.00	0.00	4.59	0.00	3.41	0.01	5.56	0.00	4.57	0.00	5.10	0.03	5.01	0.00	4.65	0.01
n21:0	0.00	0.00	0.42	0.02	0.20	0.28	0.38	0.01	0.46	0.01	0.34	0.00	0.02	0.00	0.42	0.04	0.31	0.01	0.37	0.00	0.36	0.02	0.33	0.02
C15:1	0.48	0.01	0.45	0.01	0.62	0.01	0.33	0.01	0.52	0.01	0.45	0.00	0.76	0.00	0.49	0.01	0.47	0.01	0.35	0.01	0.56	0.00	0.56	0.00
16:1ω9c	1.93	0.01	1.59	0.07	1.84	0.06	1.54	0.00	1.72	0.06	1.75	0.03	2.46	0.02	1.36	0.01	1.80	0.01	1.51	0.03	1.72	0.01	1.88	0.07
16:1ω7c	9.10	0.15	7.60	0.09	8.72	0.04	7.56	0.08	8.28	0.02	9.05	0.13	11.27	0.09	6.94	0.03	9.12	0.00	7.85	0.02	8.22	0.05	9.02	0.13
16:1ω5c	5.61	0.09	4.64	0.06	5.79	0.02	4.93	0.05	5.13	0.27	5.51	0.07	7.49	0.06	4.27	0.03	5.56	0.01	5.24	0.03	5.10	0.04	5.54	0.08
C17:1	4.25	0.06	3.30	0.13	3.96	0.17	3.13	0.01	3.78	0.02	3.93	0.14	5.07	0.01	3.24	0.00	4.10	0.03	3.44	0.00	3.70	0.03	4.16	0.11
17:1ω7c	0.53	0.01	0.51	0.06	0.54	0.04	0.41	0.02	0.56	0.00	0.50	0.06	0.80	0.00	0.36	0.02	0.45	0.01	0.46	0.00	0.56	0.01	0.57	0.01
18:1ω9c	8.40	0.16	7.07	0.01	8.26	0.03	7.00	0.07	7.47	0.00	8.27	0.05	10.53	0.00	7.23	0.01	8.51	0.00	7.40	0.01	8.02	0.02	8.52	0.06
18:1ω7c	14.25	0.27	12.28	0.01	13.86	0.06	11.98	0.12	12.87	0.01	13.69	0.07	17.38	0.00	12.45	0.02	14.80	0.00	12.29	0.02	13.93	0.04	14.06	0.09
18:1ω5c	1.20	0.03	1.02	0.00	1.21	0.00	0.98	0.01	1.10	0.01	1.18	0.00	1.74	0.00	1.01	0.01	1.25	0.01	1.09	0.00	1.24	0.00	1.29	0.01
C19:1	0.97	0.02	0.77	0.01	0.78	0.00	0.72	0.00	0.68	0.00	0.91	0.00	1.35	0.00	0.78	0.00	1.02	0.00	0.83	0.00	0.96	0.03	0.94	0.00
20:1ω9c	0.55	0.01	0.48	0.00	0.50	0.00	0.41	0.02	0.57	0.06	0.53	0.02	0.83	0.01	0.49	0.00	0.49	0.00	0.45	0.00	0.58	0.00	0.57	0.01
18:2ω6c	0.80	1.13	1.83	0.01	1.67	0.00	1.75	0.00	1.76	0.00	1.82	0.00	1.09	0.00	1.19	0.02	1.58	0.00	1.56	0.01	0.00	0.00	1.65	0.00
18:3ω3	0.19	0.27	0.78	0.01	0.21	0.00	0.50	0.00	0.27	0.00	0.42	0.00	0.18	0.00	0.13	0.05	0.33	0.01	0.52	0.00	0.00	0.00	0.27	0.00
C20:4ω6	0.23	0.32	0.60	0.01	0.47	0.00	0.50	0.00	0.56	0.00	0.70	0.00	0.40	0.00	0.49	0.00	0.63	0.00	0.38	0.01	0.00	0.00	0.48	0.00

Table A 2c: Concentration of all detected PLFAs in mol%.

	T9A	±σ	T9B	±σ	T9C	±σ	T10A	±σ	T10B	±σ	CON A	±σ	CON B	±σ	CON C	±σ
i14:0	1.80	0.00	2.02	0.00	1.93	0.02	0.89	1.21	1.98	0.01	1.94	0.01	2.03	0.02	2.20	0.01
n14:0	0.84	0.01	0.81	0.00	0.78	0.01	0.35	0.48	0.82	0.01	0.79	0.00	0.86	0.00	0.87	0.01
i15:0	6.08	0.09	6.35	0.12	6.34	0.05	2.87	3.89	6.39	0.21	6.18	0.07	6.25	0.04	7.20	0.18
a15:0	4.54	0.03	4.73	0.04	4.70	0.03	2.15	2.92	4.72	0.05	4.59	0.01	4.63	0.03	5.24	0.11
n15:0	0.40	0.00	0.31	0.00	0.30	0.00	0.14	0.20	0.34	0.00	0.30	0.00	0.32	0.00	0.32	0.00
10Me16	0.29	0.03	0.13	0.03	0.11	0.00	0.14	0.19	0.23	0.00	0.26	0.00	0.28	0.03	0.24	0.02
i16:0	1.79	0.01	1.81	0.00	1.81	0.01	0.85	1.16	1.83	0.00	1.77	0.00	1.81	0.01	1.99	0.00
n16:0	10.03	0.05	9.76	0.02	10.03	0.04	4.77	6.47	10.22	0.01	9.82	0.01	10.05	0.04	11.12	0.03
17:0br	0.70	0.00	0.72	0.00	0.71	0.00	0.35	0.47	0.74	0.00	0.67	0.04	0.67	0.01	0.77	0.00
10Me17	5.41	0.02	5.53	0.02	5.58	0.01	2.65	3.60	5.60	0.02	5.38	0.00	5.25	0.02	6.09	0.02
i17:0	1.76	0.07	1.80	0.12	1.98	0.00	0.81	1.10	1.88	0.13	1.73	0.07	1.68	0.06	1.88	0.01
a17:0	1.63	0.03	1.63	0.04	1.69	0.00	0.75	1.02	1.66	0.03	1.57	0.01	1.57	0.01	1.73	0.02
17:0cy	2.10	0.01	2.11	0.01	2.21	0.00	0.97	1.32	2.14	0.01	2.18	0.01	2.05	0.00	2.48	0.02
10Me18	0.72	0.01	0.72	0.00	0.69	0.00	0.35	0.48	0.75	0.00	0.70	0.00	0.73	0.00	0.87	0.00
n18:0	2.14	0.01	1.97	0.01	2.01	0.00	0.93	1.26	2.12	0.01	1.96	0.01	2.01	0.00	2.21	0.00
19:0br	1.10	0.01	1.10	0.00	1.09	0.01	0.54	0.73	1.11	0.01	1.12	0.00	1.13	0.00	1.29	0.00
19:0cy	5.26	0.03	5.19	0.01	5.13	0.01	2.43	3.30	5.19	0.02	5.14	0.01	5.12	0.01	5.78	0.01
n21:0	0.10	0.00	0.38	0.01	0.36	0.01	0.18	0.24	0.45	0.00	0.37	0.00	0.40	0.01	0.41	0.01
C15:1	0.70	0.01	0.64	0.00	0.68	0.01	0.24	0.33	0.74	0.00	0.74	0.01	0.49	0.29	0.78	0.01
16:1ω9c	1.58	0.03	1.46	0.03	1.50	0.08	0.68	0.92	1.56	0.02	1.58	0.00	1.55	0.04	1.72	0.00
16:1ω7c	8.08	0.13	7.39	0.10	7.67	0.06	3.41	4.64	7.79	0.01	7.88	0.03	7.87	0.01	9.17	0.02
16:1ω5c	5.02	0.08	4.62	0.06	4.69	0.05	2.44	3.32	4.97	0.26	4.94	0.01	4.93	0.01	5.92	0.01
C17:1	3.65	0.04	3.37	0.07	3.46	0.01	1.59	2.16	3.57	0.01	3.59	0.03	3.42	0.03	3.97	0.00
17:1ω7c	0.39	0.00	0.41	0.04	0.38	0.05	0.18	0.24	0.49	0.00	0.38	0.08	0.37	0.00	0.46	0.11
18:1ω9c	7.55	0.00	7.07	0.06	7.11	0.00	3.40	4.61	7.33	0.01	7.47	0.01	7.46	0.01	8.67	0.06
18:1ω7c	13.09	0.16	11.96	0.10	11.87	0.02	5.71	7.75	12.21	0.02	12.87	0.01	13.10	0.01	14.21	0.22
18:1ω5c	1.14	0.02	1.06	0.00	1.06	0.01	0.55	0.75	1.16	0.01	1.11	0.00	1.11	0.00	1.13	0.04
C19:1	0.86	0.01	0.77	0.00	0.74	0.01	0.37	0.50	0.82	0.00	0.83	0.00	0.78	0.00	0.87	0.01
20:1ω9c	0.46	0.01	0.46	0.01	0.42	0.00	0.23	0.31	0.49	0.00	0.48	0.00	0.45	0.00	0.41	0.01
18:2ω6c	1.27	0.01	1.42	0.00	1.26	0.01	0.54	0.73	1.50	0.00	1.02	0.01	1.87	0.00	2.29	0.18
18:3ω3	0.00	0.00	0.00	0.00	0.13	0.00	0.07	0.09	0.11	0.00	0.28	0.00	0.21	0.00	0.28	0.01
C20:4ω6	0.41	0.00	0.55	0.00	0.43	0.00	0.20	0.28	0.41	0.00	0.36	0.00	0.55	0.00	0.00	0.00

Table A 3a: Concentration of the analyzed PLFAs and NLFAs in mol g^{-1}

	T1A	±σ	T1B	±σ	T1C	±σ	T2A	±σ	T2B	±σ	T2C	±σ	T3A	±σ	T3B	±σ	T3C	±σ	T4A	±σ	T4B	±σ	T4C	±σ
i14:0	0.89	0.02	0.72	0.01	0.62	0.00	0.55	0.00	0.04	0.00	0.91	0.01	0.47	0.00	1.12	0.01	0.69	0.00	1.63	0.00	1.18	0.02	1.68	0.02
n14:0	0.34	0.01	0.25	0.00	0.20	0.00	0.16	0.00	0.00	0.00	0.34	0.00	0.15	0.00	0.41	0.01	0.22	0.00	0.64	0.01	0.45	0.00	0.67	0.01
i15:0	2.96	0.06	2.45	0.07	2.09	0.01	1.90	0.03	1.00	0.00	3.14	0.04	1.78	0.01	3.74	0.01	2.40	0.01	5.34	0.03	4.12	0.05	5.28	0.22
a15:0	2.35	0.05	1.78	0.02	1.54	0.01	1.39	0.01	0.73	0.00	2.28	0.02	1.32	0.01	2.76	0.01	1.77	0.00	4.01	0.02	3.03	0.03	3.91	0.09
i16:0	0.89	0.01	0.63	0.00	0.55	0.00	0.48	0.00	0.37	0.00	0.86	0.01	0.47	0.01	1.06	0.01	0.62	0.01	1.55	0.00	1.15	0.01	1.52	0.01
n16:0	4.77	0.07	3.89	0.02	3.34	0.02	3.09	0.02	2.75	0.01	5.03	0.02	2.89	0.02	5.83	0.02	3.51	0.01	7.89	0.05	5.85	0.05	7.95	0.07
17:0br	0.28	0.00	0.20	0.01	0.18	0.00	0.13	0.00	0.10	0.00	0.28	0.00	0.12	0.00	0.34	0.02	0.16	0.00	0.52	0.01	0.38	0.00	0.50	0.00
10Me17:0	2.60	0.03	2.09	0.01	1.86	0.01	1.61	0.01	1.62	0.00	2.65	0.01	1.63	0.09	3.19	0.01	1.94	0.01	4.32	0.03	3.24	0.01	4.50	0.04
i17:0	0.83	0.05	0.63	0.00	0.53	0.01	0.48	0.01	0.49	0.00	0.82	0.01	0.46	0.00	1.01	0.01	0.58	0.00	1.39	0.01	1.06	0.01	1.61	0.01
a17:0	0.75	0.02	0.57	0.00	0.49	0.00	0.42	0.00	0.42	0.00	0.72	0.00	0.39	0.00	0.89	0.01	0.50	0.00	1.26	0.00	0.93	0.01	1.38	0.01
17:0cy	0.96	0.01	0.78	0.01	0.66	0.00	0.59	0.01	0.56	0.00	1.01	0.00	0.54	0.00	1.20	0.01	0.71	0.01	1.66	0.00	1.28	0.00	1.75	0.01
10Me18:0	0.32	0.00	0.22	0.00	0.19	0.00	0.15	0.00	0.18	0.00	0.28	0.00	0.14	0.00	0.41	0.00	0.23	0.01	0.62	0.01	0.46	0.00	0.60	0.00
n18:0	0.95	0.00	0.74	0.00	0.61	0.00	0.55	0.00	0.66	0.00	0.92	0.00	0.52	0.00	1.11	0.00	0.61	0.00	1.51	0.01	1.10	0.00	1.58	0.00
19:0br	0.53	0.00	0.39	0.00	0.32	0.00	0.29	0.00	0.36	0.00	0.48	0.01	0.28	0.00	0.64	0.01	0.37	0.00	0.92	0.01	0.70	0.00	0.92	0.00
19:0cy	2.64	0.01	1.99	0.00	1.66	0.00	1.50	0.01	1.75	0.01	2.48	0.01	1.37	0.00	2.90	0.01	1.71	0.01	3.84	0.00	2.85	0.00	4.07	0.00
C15:1	0.30	0.00	0.25	0.00	0.22	0.00	0.08	0.06	0.22	0.00	0.01	0.00	0.08	0.00	0.24	0.00	0.44	0.01	0.39	0.00	0.27	0.00	0.51	0.11
16:1ω9c	0.60	0.00	0.55	0.00	0.46	0.01	0.41	0.03	0.93	0.01	0.32	0.02	0.46	0.01	0.81	0.02	1.39	0.02	1.31	0.02	1.05	0.03	1.32	0.03
16:1ω7c	3.12	0.03	2.98	0.02	2.53	0.04	2.10	0.02	4.57	0.06	1.87	0.00	2.57	0.01	4.13	0.02	6.60	0.19	6.11	0.03	5.32	0.04	6.12	0.04
16:1ω5c	1.95	0.02	1.79	0.01	1.50	0.03	1.22	0.00	2.86	0.03	1.15	0.00	1.55	0.01	2.51	0.02	3.96	0.11	3.73	0.02	3.16	0.03	3.77	0.02
C17:1	1.60	0.00	1.36	0.00	1.19	0.06	0.92	0.00	1.97	0.10	0.95	0.00	1.15	0.01	1.92	0.01	3.05	0.07	2.65	0.10	2.38	0.02	2.78	0.01
18:1ω9c	3.10	0.00	2.76	0.04	2.33	0.01	1.94	0.00	4.14	0.02	2.45	0.01	2.43	0.01	3.89	0.01	6.05	0.07	5.67	0.01	4.65	0.01	5.78	0.02
18:1ω7c	5.08	0.04	4.70	0.11	3.97	0.05	3.33	0.00	7.11	0.03	4.10	0.02	4.03	0.02	6.45	0.01	9.97	0.11	9.50	0.01	7.66	0.02	9.69	0.04
18:1ω5c	0.40	0.01	0.36	0.01	0.30	0.01	0.21	0.00	0.59	0.00	0.31	0.00	0.28	0.00	0.55	0.00	0.86	0.00	0.81	0.00	0.61	0.01	0.89	0.00
C19:1	0.30	0.00	0.27	0.00	0.22	0.00	0.16	0.00	0.43	0.00	0.24	0.00	0.22	0.01	0.39	0.00	0.67	0.00	0.54	0.00	0.54	0.00	0.63	0.01
18:2ω6c	0.62	0.00	0.63	0.00	0.40	0.02	0.39	0.00	0.41	0.00	0.83	0.01	0.55	0.01	0.81	0.00	1.17	0.13	1.18	0.00	0.87	0.01	1.04	0.00
16:1ω5NLFA	3.92	0.02	4.32	0.00	2.97	0.00	4.49	0.01	4.64	0.03	6.78	0.02	3.70	0.02	5.86	0.01	4.97	0.04	5.42	0.02	4.72	0.03	3.16	0.03

Table A 3b: Concentration of the analyzed PLFAs and NLFAs in mol g^{-1}

	T5A	±σ	T5B	±σ	T5C	±σ	T6A	±σ	T6B	±σ	T6C	±σ	T7A	±σ	T7B	±σ	T7C	±σ	T8A	±σ	T8B	±σ	T8C	±σ
i14:0	0.89	0.00	1.34	0.00	1.00	0.01	0.98	0.03	1.82	0.03	0.85	0.00	0.86	0.00	0.64	0.00	0.72	0.00	0.99	0.01	1.19	0.00	0.93	0.00
n14:0	0.33	0.01	0.50	0.00	0.36	0.00	0.41	0.01	0.74	0.01	0.35	0.00	0.35	0.00	0.29	0.00	0.29	0.00	0.40	0.00	0.48	0.00	0.37	0.00
i15:0	3.05	0.02	4.27	0.06	3.22	0.02	3.24	0.13	5.85	0.08	2.76	0.03	2.81	0.01	2.63	0.02	2.25	0.00	3.28	0.03	3.89	0.01	3.19	0.07
a15:0	2.31	0.01	3.14	0.04	2.35	0.00	2.42	0.06	4.26	0.06	2.00	0.02	2.07	0.00	1.97	0.01	1.66	0.00	2.43	0.02	2.89	0.01	2.33	0.03
i16:0	0.83	0.00	1.24	0.00	0.92	0.00	0.95	0.02	1.66	0.01	0.78	0.00	0.79	0.00	0.85	0.00	0.65	0.00	0.95	0.00	1.14	0.01	0.89	0.00
n16:0	4.53	0.01	6.38	0.00	4.85	0.01	5.06	0.06	8.52	0.06	4.22	0.00	4.37	0.00	4.70	0.02	3.60	0.01	4.94	0.02	5.99	0.02	4.77	0.01
17:0br	0.29	0.00	0.41	0.00	0.31	0.00	0.35	0.01	0.61	0.00	0.29	0.00	0.31	0.00	0.32	0.00	0.25	0.00	0.35	0.00	0.41	0.00	0.35	0.00
10Me17:0	2.58	0.02	3.42	0.00	2.65	0.01	2.69	0.04	4.59	0.01	2.25	0.00	2.43	0.00	2.54	0.01	1.97	0.00	2.75	0.01	3.20	0.01	2.74	0.01
i17:0	0.79	0.00	1.14	0.00	0.90	0.06	0.89	0.01	1.54	0.03	0.75	0.00	0.79	0.00	0.86	0.00	0.61	0.00	0.93	0.00	1.10	0.01	0.90	0.02
a17:0	0.70	0.00	1.01	0.00	0.79	0.02	0.80	0.01	1.37	0.01	0.67	0.00	0.70	0.00	0.78	0.00	0.57	0.00	0.80	0.00	0.96	0.00	0.78	0.00
17:0cy	1.01	0.00	1.37	0.00	1.07	0.01	1.07	0.02	1.86	0.01	0.89	0.00	0.94	0.01	0.99	0.01	0.76	0.01	1.06	0.00	1.29	0.00	1.08	0.00
10Me18:0	0.29	0.00	0.46	0.00	0.36	0.00	0.39	0.01	0.71	0.00	0.33	0.00	0.28	0.00	0.34	0.00	0.24	0.00	0.38	0.00	0.44	0.00	0.35	0.00
n18:0	0.88	0.00	1.25	0.00	0.95	0.00	0.98	0.01	1.67	0.00	0.83	0.00	0.88	0.00	0.99	0.00	0.71	0.00	0.98	0.00	1.19	0.00	0.95	0.00
19:0br	0.50	0.00	0.77	0.00	0.58	0.00	0.61	0.01	1.06	0.00	0.49	0.00	0.48	0.00	0.58	0.01	0.40	0.00	0.58	0.00	0.70	0.00	0.56	0.00
19:0cy	2.55	0.01	3.37	0.00	2.60	0.00	2.60	0.02	4.32	0.00	2.15	0.00	2.26	0.00	2.56	0.00	1.94	0.00	2.53	0.00	3.07	0.00	2.52	0.00
C15:1	0.23	0.01	0.28	0.01	0.34	0.01	0.17	0.00	0.45	0.01	0.21	0.00	0.50	0.00	0.22	0.01	0.20	0.00	0.17	0.00	0.34	0.00	0.30	0.00
16:1ω9c	0.93	0.02	0.99	0.05	1.00	0.03	0.80	0.01	1.48	0.05	0.82	0.01	1.62	0.02	0.63	0.00	0.76	0.01	0.75	0.02	1.05	0.01	1.02	0.04
16:1ω7c	4.40	0.02	4.75	0.07	4.73	0.01	3.91	0.01	7.14	0.01	4.23	0.06	7.46	0.09	3.20	0.01	3.86	0.00	3.89	0.01	5.03	0.04	4.90	0.08
16:1ω5c	2.71	0.01	2.90	0.05	3.14	0.00	2.55	0.01	4.42	0.23	2.58	0.04	4.95	0.06	1.97	0.01	2.36	0.00	2.60	0.00	3.12	0.03	3.01	0.05
C17:1	2.05	0.01	2.07	0.07	2.15	0.10	1.62	0.01	3.26	0.02	1.84	0.06	3.35	0.01	1.49	0.00	1.74	0.01	1.71	0.01	2.26	0.02	2.26	0.05
18:1ω9c	4.06	0.01	4.42	0.02	4.48	0.00	3.62	0.01	6.45	0.01	3.87	0.02	6.96	0.02	3.33	0.00	3.61	0.00	3.67	0.02	4.91	0.01	4.62	0.04
18:1ω7c	6.89	0.02	7.68	0.03	7.51	0.01	6.19	0.01	11.10	0.02	6.41	0.03	11.50	0.04	5.73	0.01	6.27	0.00	6.10	0.04	8.53	0.03	7.63	0.07
18:1ω5c	0.58	0.00	0.64	0.01	0.65	0.00	0.51	0.00	0.95	0.00	0.55	0.00	1.15	0.00	0.47	0.00	0.53	0.00	0.54	0.00	0.76	0.00	0.70	0.00
C19:1	0.47	0.00	0.48	0.00	0.42	0.00	0.37	0.00	0.59	0.00	0.43	0.00	0.89	0.00	0.36	0.00	0.43	0.00	0.41	0.00	0.59	0.02	0.51	0.00
18:2ω6c	0.39	0.56	1.15	0.01	0.91	0.00	0.91	0.01	1.52	0.00	0.85	0.00	0.72	0.00	0.55	0.01	0.67	0.00	0.77	0.01	0.00	0.00	0.90	0.00
16:1ω5NLFA	3.17	0.01	5.03	0.00	4.75	0.03	6.18	0.01	5.76	0.01	4.02	0.01	4.98	0.03	6.03	0.00	4.21	0.00	4.28	0.01	5.38	0.01	4.22	0.03

Table A 3c: Concentration of the analyzed PLFAs and NLFAs in mol g^{-1}

	T9A	±σ	T9B	±σ	T9C	±σ	T10A	±σ	T10B	±σ	CON A	±σ	CON B	±σ	CON C	±σ
i14:0	0.79	0.00	1.00	0.00	0.79	0.01	0.95	0.01	1.14	0.01	0.85	0.01	0.93	0.01	0.69	0.00
n14:0	0.37	0.00	0.40	0.00	0.32	0.00	0.37	0.00	0.47	0.01	0.34	0.00	0.39	0.00	0.27	0.00
i15:0	2.66	0.05	3.14	0.06	2.61	0.01	3.02	0.03	3.67	0.13	2.71	0.02	2.87	0.02	2.27	0.05
a15:0	1.98	0.02	2.34	0.02	1.93	0.01	2.27	0.02	2.71	0.04	2.01	0.00	2.13	0.02	1.65	0.03
i16:0	0.78	0.00	0.89	0.00	0.74	0.00	0.91	0.00	1.05	0.00	0.77	0.00	0.83	0.00	0.62	0.00
n16:0	4.38	0.00	4.83	0.00	4.13	0.01	5.08	0.02	5.87	0.02	4.30	0.00	4.62	0.03	3.50	0.00
17:0br	0.31	0.00	0.36	0.00	0.29	0.00	0.37	0.00	0.43	0.00	0.29	0.02	0.31	0.00	0.24	0.00
10Me17:0	2.36	0.00	2.74	0.01	2.30	0.00	2.82	0.00	3.21	0.01	2.36	0.00	2.41	0.01	1.91	0.00
i17:0	0.77	0.03	0.89	0.06	0.81	0.00	0.88	0.03	1.08	0.08	0.76	0.03	0.77	0.03	0.59	0.00
a17:0	0.71	0.02	0.81	0.02	0.70	0.00	0.80	0.00	0.95	0.02	0.69	0.00	0.72	0.01	0.54	0.00
17:0cy	0.92	0.00	1.04	0.01	0.91	0.00	1.03	0.00	1.23	0.01	0.95	0.00	0.94	0.00	0.78	0.00
10Me18:0	0.31	0.00	0.36	0.00	0.28	0.00	0.38	0.00	0.43	0.00	0.31	0.00	0.34	0.00	0.28	0.00
n18:0	0.93	0.00	0.97	0.00	0.83	0.00	0.99	0.00	1.22	0.00	0.86	0.00	0.92	0.00	0.69	0.00
19:0br	0.48	0.00	0.54	0.00	0.45	0.00	0.57	0.00	0.64	0.00	0.49	0.00	0.52	0.00	0.40	0.00
19:0cy	2.30	0.00	2.57	0.00	2.11	0.00	2.58	0.00	2.98	0.00	2.25	0.00	2.35	0.00	1.82	0.00
C15:1	0.30	0.00	0.32	0.00	0.28	0.00	0.26	0.00	0.42	0.00	0.32	0.00	0.22	0.13	0.25	0.00
16:1ω9c	0.69	0.02	0.72	0.01	0.62	0.03	0.71	0.02	0.89	0.01	0.69	0.00	0.71	0.02	0.54	0.00
16:1ω7c	3.53	0.04	3.66	0.05	3.15	0.03	3.60	0.04	4.47	0.03	3.45	0.02	3.62	0.00	2.88	0.02
16:1ω5c	2.19	0.02	2.29	0.03	1.93	0.02	2.57	0.03	2.85	0.13	2.16	0.01	2.27	0.00	1.86	0.01
C17:1	1.59	0.01	1.67	0.03	1.42	0.01	1.68	0.02	2.05	0.02	1.57	0.01	1.57	0.02	1.25	0.01
18:1ω9c	3.30	0.02	3.50	0.02	2.93	0.01	3.60	0.02	4.21	0.01	3.27	0.00	3.43	0.01	2.73	0.03
18:1ω7c	5.72	0.10	5.91	0.04	4.88	0.01	6.04	0.03	7.01	0.02	5.64	0.00	6.02	0.01	4.47	0.09
18:1ω5c	0.50	0.01	0.52	0.00	0.43	0.00	0.59	0.00	0.67	0.01	0.49	0.00	0.51	0.00	0.35	0.01
C19:1	0.37	0.00	0.38	0.00	0.30	0.00	0.39	0.00	0.47	0.00	0.36	0.00	0.36	0.00	0.27	0.00
18:2ω6c	0.56	0.01	0.70	0.00	0.52	0.00	0.57	0.00	0.86	0.00	0.45	0.00	0.86	0.00	0.72	0.06
16:1ω5NLFA	3.98	0.03	5.81	0.05	4.57	0.01	9.76	0.14	4.99	0.06	4.39	0.03	4.14	0.02	4.56	0.03

Table A 4a: Isotopes values after offset correction.

	10MeC17:0	±σ	i14:0	±σ	a15:0	±σ	i15:0	±σ	i16:0	±σ	n16:0	±σ	a17:0	±σ	17:0cy	±σ
T1A	-28.57	0.16	-30.09	0.33	-21.37	0.15	-22.57	0.26	-15.94	0.32	23.36	0.20	-19.27	0.21	-28.97	0.37
T1B	-28.76	0.30	-24.99	0.58	-16.47	0.22	-18.99	0.02	-6.90	0.35	102.67	0.26	-14.45	0.95	-29.05	0.40
T1C	-27.73	0.16	-26.41	0.28	-18.26	0.37	-20.35	0.15	-12.26	0.33	51.94	0.30	-18.47	0.34	-28.59	1.15
T2A	-27.76	0.27	-23.01	0.18	-16.37	0.16	-18.51	0.43	-7.73	0.38	65.83	0.36	-15.93	0.96	-27.48	0.25
T2B	-28.99	0.11	n.d.	-	-17.42	0.64	-25.11	0.07	-13.99	0.54	78.43	0.33	-16.17	0.36	-28.80	0.16
T2C	-28.56	0.09	-27.53	1.20	-18.33	0.14	-20.23	0.19	-11.32	0.12	101.22	0.08	-16.02	0.32	-28.98	0.59
T3A	-28.11	0.29	-25.25	0.29	-17.50	0.69	-20.74	0.07	-13.46	0.38	77.12	0.19	-17.24	0.30	-27.83	0.91
T3B	-28.39	0.29	-23.56	0.27	-16.99	0.09	-18.20	0.11	-9.73	0.16	100.39	0.60	-16.78	0.71	-28.19	0.54
T3C	-28.61	0.08	-23.75	0.87	-17.24	0.73	-20.54	0.33	-13.40	0.56	87.03	0.13	-17.25	0.15	-29.26	0.71
T4A	-27.94	0.19	-23.45	0.32	-18.04	0.25	-18.48	0.27	-13.19	0.47	92.23	0.49	-17.06	0.71	-27.24	0.34
T4B	-27.68	0.23	-23.42	0.54	-18.36	0.30	-19.79	0.34	-14.92	0.40	62.26	0.26	-17.86	0.50	-28.55	0.73
T4C	-28.33	0.39	-27.32	0.11	-22.11	0.21	-21.38	0.15	-18.89	0.32	54.55	0.27	-21.38	0.09	-27.90	0.43
T5A	-27.07	0.46	-21.45	0.22	-15.79	0.11	-17.35	0.09	-10.94	0.31	68.12	0.28	-16.20	0.45	-23.57	0.32
T5B	-27.16	0.12	-19.15	0.37	-16.00	0.10	-16.10	0.46	-12.75	0.26	86.27	0.40	-15.98	0.57	-23.82	0.29
T5C	-27.54	0.69	-21.55	0.20	-15.94	0.07	-16.07	0.15	-13.46	0.10	96.65	0.15	-15.95	0.14	-23.01	0.52
T6A	-26.24	0.36	-18.34	0.20	-14.26	0.08	-14.08	0.03	-11.83	0.33	86.58	0.16	-14.27	0.46	-15.82	0.12
T6B	-25.85	0.16	-4.83	0.06	-7.73	0.10	-7.29	0.26	-5.34	0.28	80.97	0.08	-10.70	0.45	-20.40	0.22
T6C	-26.17	0.08	-17.56	0.24	-14.50	0.23	-14.16	0.28	-13.53	0.62	69.42	0.21	-15.72	0.38	-18.55	0.31
T7A	-24.91	0.50	-14.14	0.15	-9.62	0.23	-6.74	0.07	-9.04	0.34	41.15	0.08	-12.08	0.54	-14.11	0.20
T7B	-24.85	0.45	-9.59	0.48	-6.98	0.25	-4.52	0.06	-7.85	0.60	60.45	0.16	-10.64	0.59	-8.10	0.33
T7C	-23.35	0.16	-6.68	0.72	-7.39	0.38	-4.34	0.16	-7.59	0.35	43.11	0.23	-10.41	0.35	-14.07	0.61
T8A	-22.63	0.28	-15.36	0.17	-11.41	0.08	-8.00	0.36	-10.91	0.38	23.93	0.14	-13.33	0.11	-7.08	0.13
T8B	-23.40	1.83	-8.87	0.16	-5.46	0.19	-0.66	0.01	-5.13	0.14	38.64	0.10	-8.43	0.21	-4.61	0.33
T8C	-22.70	0.14	-8.51	0.25	-4.31	0.23	0.88	0.14	-4.43	0.43	32.46	0.24	-9.24	0.60	-2.52	0.22
T9A	-18.99	1.01	-6.04	0.26	0.30	0.31	7.02	0.25	0.87	0.35	37.86	0.18	-4.66	1.51	5.24	0.22
T9B	-19.08	0.55	-7.66	0.25	-2.28	0.52	2.37	0.43	-3.00	0.32	28.27	0.40	-7.00	0.40	1.39	2.90
T9C	-23.53	0.27	-17.01	0.19	-11.66	0.09	-8.58	0.15	-11.25	0.19	8.33	0.20	-13.80	0.17	-8.68	0.39
T10A	-22.90	0.25	-17.53	0.22	-8.69	0.12	-6.21	0.21	-7.43	0.44	32.46	0.29	-9.92	0.28	-11.90	0.20
T10B	-19.77	0.52	-9.99	0.25	-1.38	0.42	2.53	0.08	-1.67	0.30	26.30	0.38	-5.05	0.11	5.76	0.33
CON A	-28.39	0.75	-29.06	0.19	-25.28	0.08	-26.62	0.13	-25.47	0.23	-26.65	0.18	-25.27	0.36	-28.24	0.40
CON B	-28.94	0.33	-30.28	0.37	-26.82	0.30	-27.75	0.15	-27.13	0.44	-28.56	0.05	-26.43	0.83	-29.59	0.35
CON C	-28.48	0.18	-29.14	0.34	-26.09	0.05	-27.04	0.13	-26.19	0.09	-27.24	0.31	-25.46	0.29	-28.58	0.33

Table A 4b: Isotopes values after offset correction.

	C17:0i	±σ	C18:0n	±σ	C19:0cy	±σ	16:1ω5	±σ	16:1ω7c	±σ	16:1ω9c	±σ	18:1ω5c	±σ	18:1ω7c	±σ
T1A	-19.17	0.31	12.37	0.21	-32.66	0.38	-23.42	0.09	-9.66	0.21	-19.10	0.82	-18.92	0.53	-4.02	0.44
T1B	-13.26	0.53	30.03	0.53	-30.74	0.31	-20.02	0.40	-1.00	0.34	-16.98	0.46	-12.31	0.76	18.59	0.07
T1C	-15.07	0.60	9.24	0.38	-30.60	1.33	-22.22	0.06	-5.74	0.04	-20.15	3.01	-17.76	0.71	3.62	0.06
T2A	-11.69	0.50	11.20	0.79	-40.15	0.60	-20.92	0.06	-0.54	0.12	-16.84	1.10	-23.24	5.88	12.22	0.09
T2B	-13.61	0.50	10.64	0.74	-31.34	0.21	-18.53	0.47	4.25	0.47	-11.74	0.73	-11.66	0.69	12.95	0.37
T2C	-14.72	0.33	10.49	0.38	-31.29	0.31	39.12	0.2	-5.72	0.71	-16.99	0.38	-7.83	1.39	10.31	0.27
T3A	-14.36	0.13	10.66	0.69	-30.59	0.38	-19.79	0.07	-0.22	0.07	-16.20	0.38	-20.30	6.95	10.75	0.35
T3B	-12.41	0.38	15.94	0.27	-30.85	0.51	-18.31	0.06	19.58	0.15	-11.27	0.29	-12.95	0.38	24.53	0.16
T3C	-14.34	0.22	12.57	1.18	-37.75	6.25	-19.58	0.23	2.23	0.24	-14.47	1.42	-13.79	0.65	10.05	0.06
T4A	-13.44	0.26	11.00	0.40	-30.50	0.63	-5.90	1.77	8.72	0.21	-14.79	2.03	-11.16	0.41	12.41	0.26
T4B	-15.08	0.37	5.48	0.14	-30.48	0.21	-18.99	0.06	-1.34	0.06	-14.95	0.64	-17.04	0.59	4.25	0.18
T4C	-18.80	0.08	1.07	0.32	-31.99	1.03	2.20	0.32	-2.11	0.19	-18.39	0.11	-14.25	0.31	3.32	0.28
T5A	-12.69	0.10	8.80	0.44	-29.33	0.57	-16.29	0.21	14.04	0.31	-11.63	0.42	-11.78	0.37	11.30	0.11
T5B	-12.31	0.44	18.37	0.40	-30.09	0.37	-13.30	0.13	24.18	0.20	-10.74	1.78	-13.98	0.36	15.85	0.19
T5C	-12.26	0.51	12.79	0.52	-30.01	0.32	-11.75	0.17	30.17	0.10	-7.85	0.88	-14.50	0.26	17.70	0.04
T6A	-10.99	0.12	14.10	0.22	-28.89	0.55	-9.24	0.10	32.31	0.11	-7.97	1.10	-13.14	0.61	16.24	0.27
T6B	-5.94	0.36	20.15	0.34	-28.54	0.54	-0.93	0.15	31.88	0.47	8.11	2.05	-8.30	0.66	21.72	0.39
T6C	-11.16	0.64	10.89	0.21	-28.81	0.16	-9.34	0.16	20.70	0.14	-7.77	0.89	-14.95	0.38	12.28	0.21
T7A	-5.84	0.36	8.77	0.19	-27.18	0.17	-1.07	0.17	17.70	0.13	1.50	1.48	-13.03	0.67	9.95	0.18
T7B	-2.84	0.31	18.35	0.20	-25.47	0.47	8.20	0.26	30.21	0.09	5.83	0.38	-8.01	1.12	19.68	0.26
T7C	-3.91	0.24	17.29	0.14	-24.95	0.16	11.56	0.06	18.10	0.27	5.56	0.36	-7.53	0.88	14.55	0.26
T8A	-7.56	0.19	4.94	0.56	-24.77	0.16	1.36	0.09	7.11	0.16	-1.25	0.18	-14.28	0.35	1.12	0.16
T8B	-1.67	0.14	15.60	0.45	-22.70	0.87	13.81	0.12	15.47	0.20	8.40	0.77	-8.68	0.90	12.70	0.05
T8C	-0.91	0.41	15.56	0.09	-23.32	0.36	12.29	0.12	17.72	0.18	11.04	1.35	-9.67	0.49	8.91	0.25
T9A	3.94	0.31	15.86	0.35	-17.34	0.51	21.47	0.07	19.08	0.09	12.06	0.98	-4.04	0.36	16.33	0.23
T9B	0.95	0.09	19.94	0.46	-22.54	4.40	14.77	0.11	12.44	0.11	8.29	1.13	-8.98	0.39	7.20	0.15
T9C	-9.25	0.35	-1.58	0.27	-24.81	1.16	-0.34	0.29	-0.19	0.14	-5.86	1.52	-14.71	1.55	-3.62	0.06
T10A	-7.39	0.21	2.16	0.20	-25.07	0.10	52.95	0.16	3.39	0.14	-5.22	2.41	-5.20	0.41	10.91	0.24
T10B	0.55	0.40	10.76	0.23	-18.39	1.17	12.75	0.08	12.85	0.06	7.28	2.08	-6.87	0.71	10.43	0.30
CON A	-26.19	0.19	-25.46	0.27	-32.77	0.27	-25.56	0.13	-28.96	0.04	-26.03	2.66	-22.52	0.25	-28.34	0.21
CON B	-27.77	0.50	-27.68	0.24	-31.10	0.65	-26.97	0.10	-29.85	0.13	-25.27	1.26	-24.18	0.46	-29.37	0.22
CON C	-26.44	0.16	-26.37	0.24	-30.99	0.50	-26.18	0.04	-29.13	0.42	-25.86	1.08	-23.73	0.60	-28.77	0.30

Table A 4c: Isotopes values after offset correction.

	18:1ω9c	±σ	18:2ω6,9	±σ	16:1ω5 NLFA	±σ
T1A	1.66	0.55	149.66	0.02	32.62	0.20
T1B	17.18	0.12	434.09	1.23	55.52	0.45
T1C	0.39	0.45	223.80	0.79	39.26	0.38
T2A	0.55	0.37	398.29	2.13	39.48	0.18
T2B	4.79	1.00	373.19	1.74	47.78	0.04
T2C	-2.52	0.65	325.93	0.27	653.89	1.73
T3A	2.43	0.10	452.24	1.11	62.31	0.18
T3B	4.23	0.61	582.68	1.99	67.85	0.25
T3C	-5.56	0.83	645.96	1.09	47.98	0.09
T4A	-10.41	0.56	518.46	1.76	109.60	0.29
T4B	-11.49	0.32	502.65	1.69	32.80	0.22
T4C	-15.20	0.97	263.18	0.89	150.93	0.14
T5A	-10.59	0.45	613.31	0.06	69.40	0.14
T5B	-4.37	0.17	572.85	1.08	85.56	0.18
T5C	-8.56	0.27	699.08	1.02	80.39	0.16
T6A	-10.61	0.25	574.20	3.17	71.32	4.44
T6B	-10.98	0.25	692.93	0.90	55.66	5.40
T6C	-11.62	0.16	502.44	1.31	59.73	0.15
T7A	-13.71	0.24	328.88	1.11	28.26	0.31
T7B	-9.90	0.37	332.46	1.00	43.05	0.16
T7C	-10.45	0.67	265.10	0.25	68.53	2.52
T8A	-14.12	0.58	158.43	0.73	0.93	0.40
T8B	-9.35	0.34	n.d.	-	18.76	0.82
T8C	-10.75	0.61	193.69	0.11	7.35	0.36
T9A	-9.44	0.47	189.54	0.80	7.94	0.27
T9B	-9.62	0.38	155.96	0.07	-2.04	0.20
T9C	-17.29	0.67	70.43	0.34	-14.44	0.16
T10A	-11.44	0.22	72.30	0.59	284.84	1.08
T10B	-11.67	0.09	117.21	0.19	2.85	0.31
CON A	-27.52	0.25	-25.45	0.06	-28.77	0.28
CON B	-27.96	0.87	-30.98	0.13	-29.10	0.15
CON C	-27.66	0.41	n.d.	-	-29.19	0.17

Table A 5a: ^{13}C enrichment in C nmol g^{-1}.

time	18:2w6,9	±σ	16:1w5 NLFA	±σ	16:1w5 PLFA	±σ	18:1w9	±σ	10Me17:0	±σ	16:0n	±σ	18:0n	±σ	14:0i	±σ
1	167.55	91.96	269.67	66.96	7.54	3.15	93.51	28.79	0.46	1.01	338.03	167.82	33.54	11.46	1.53	1.76
3	209.48	96.52	331.90	2291.87	67.36	95.31	79.50	33.83	0.13	0.95	324.83	274.03	25.13	7.81	2.68	2.24
12	515.09	206.97	429.68	108.48	18.76	8.80	110.51	52.99	0.49	0.56	483.34	189.66	30.15	13.06	4.20	1.99
24	470.45	164.34	537.26	290.14	68.71	39.88	81.97	16.44	2.36	1.32	707.13	186.35	45.23	10.92	6.87	3.48
48	533.18	257.57	469.22	114.96	36.65	7.31	86.12	14.48	3.90	0.96	586.81	134.26	41.54	9.33	9.62	2.57
96	697.02	259.54	488.43	113.57	66.23	27.62	77.31	26.17	8.14	3.26	636.85	250.46	49.58	20.01	21.97	14.12
168	216.89	38.70	376.78	122.09	93.83	52.71	73.00	33.17	9.61	2.37	322.47	62.47	35.51	7.25	14.08	3.46
336	171.48	27.50	179.53	49.56	104.19	22.30	72.81	15.33	16.39	1.93	312.02	55.40	40.29	8.27	19.39	4.77
504	100.66	40.57	123.56	58.16	82.78	25.26	51.33	15.45	20.13	6.77	234.46	70.07	35.13	11.00	16.71	5.64
672	91.23	35.11	159.10	1998.53	157.56	106.90	62.99	36.83	22.22	13.77	310.01	183.49	36.87	22.16	16.75	10.52

	15:0a	±σ	15:0i	±σ	16:0i	±σ	17:0a	±σ	17:0i	±σ	16:1w7	±σ	18:1w7	±σ	17:0cy	±σ
1	13.39	5.38	15.88	5.22	9.67	3.90	4.95	1.89	7.00	2.53	68.48	14.46	159.27	56.02	-0.07	-0.26
3	13.26	5.87	12.71	12.59	10.22	3.57	5.25	1.51	12.87	7.87	76.99	42.74	195.46	80.83	0.20	1.17
12	17.35	6.58	20.22	8.61	10.50	4.77	5.17	2.29	9.16	3.91	161.59	88.06	297.10	141.42	0.31	0.63
24	23.66	8.89	35.63	8.71	14.81	4.72	8.08	3.11	14.63	4.68	182.62	38.29	318.89	60.19	1.50	1.11
48	26.36	4.80	37.56	7.49	13.75	3.24	8.08	1.54	13.59	2.55	242.11	39.28	322.98	30.44	6.10	1.12
96	43.27	21.56	64.72	31.96	19.45	9.55	12.14	5.41	19.34	8.33	296.46	108.97	367.85	134.67	12.86	5.92
168	34.25	4.67	56.07	7.14	13.77	1.95	9.98	1.65	17.06	3.07	241.33	119.07	332.00	139.91	15.18	3.79
336	48.60	11.25	85.05	18.90	19.41	4.33	13.14	2.72	22.94	4.37	199.14	37.41	274.84	63.73	27.60	4.07
504	45.23	14.07	77.27	24.00	17.72	5.31	12.81	3.67	20.87	5.89	138.47	35.67	198.10	59.21	26.98	7.22
672	53.13	31.96	86.01	52.62	21.44	12.68	16.12	9.70	23.30	14.30	153.05	92.27	257.57	149.76	29.98	20.21

Table A 5b: ^{13}C enrichment in C nmol g^{-1}.

	19:0cy	±σ	16:1w9	±σ	18:1w5	±σ
1	0.23	0.93	3.80	1.02	2.53	1.30
3	-3.95	-7.04	5.41	3.55	4.29	4.36
12	-2.29	-6.49	10.59	6.05	5.01	3.68
24	2.00	2.79	11.77	2.86	7.37	2.68
48	5.06	1.43	15.28	2.01	6.24	0.98
96	8.80	3.38	26.30	14.40	8.11	3.84
168	12.89	3.17	29.26	15.98	9.21	5.26
336	21.87	3.84	30.54	8.21	8.63	2.52
504	23.49	9.25	21.01	6.71	7.01	2.71
672	28.14	20.85	21.98	14.20	10.88	6.19

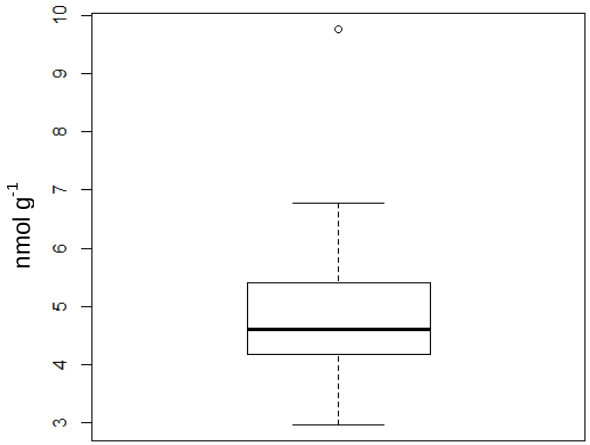

Figure A1: Boxplot of the NLFA concentrations. The big line indicates the median; the upper and lower margin of the rectangle indicates the upper and lower quartile. The end of the lines displays the upper and lower Whiskers; the dot exhibits an outlier.

Erklärung

Ich versichere hiermit, dass die vorliegende Masterarbeit selbstständig verfasst und keine weiteren als die angegebenen Hilfsmittel benutzt sowie die Stellen der Arbeit, die in anderen Werken dem Wortlaut oder dem Sinn nach entnommen sind, durch Angaben der Quellen sichtbar gemacht wurden.

Ort/Datum: _____

Unterschrift: _____